[10,11]. It is therefore clinically very important to clarify the regulatory mechanism(s) of GLUT4 expression in adipose tissues.

To examine the regulatory mechanism(s) of GLUT4 expression and identify the high-fat responsive elements (HFRE) in the GLUT4 gene, we have previously produced transgenic mice expressing mouse GLUT4 minigenes containing 5′-deletions of the GLUT4 5′-flanking region [12]. These GLUT4 minigenes contain different lengths of 5′-flanking sequence, all exons and introns, and 1 kb of 3′-flanking sequence of the GLUT4 gene, as well as a segment of foreign DNA (281 bp) inserted in the 3′-untranslated region for transcript identification [13]. In our previous study, skeletal muscle specific elements were located downstream of base −423, while adipose tissue specific elements (ASE) were located within 109 bp between bases −551 and −442 [14]. By high-fat diet feeding in −7396, −3238, −2001, −1001, and −442 minigene GLUT4 transgenic mice, HFRE were found to be located within 559 bp between bases −1001 and −442 of the mouse GLUT4 of 5′-flank [12].

In this report, in confining the area for the adipose tissue specific elements located 109 bp between bases −551 and −442, −506 minigene GLUT4 transgenic mice were made and examined to determine whether transcripts from this minigene construct expressed in adipose tissues or not. In addition, to find the binding protein and putative transcription factor(s) that might be responsible for the adipose tissue specific expression of GLUT4, gel shift analysis using systematically mutated oligonucleotide and UV cross-linking analysis were performed. Furthermore, to examine whether ASE is the same or different with HFRE, the regulation of GLUT4 minigenes containing −701 and −551 bp of 5′-flanking region under high-fat diet was studied in transgenic mice.

Materials and methods

Plasmid construction. The −506 minigene GLUT4 construct was derived from the plasmid 14 kb minigene GLUT4 containing 7396 bp of GLUT4 5′-flanking DNA with a "tag" consisting of 281 bp of foreign DNA [13]. The GLUT4 minigene constructs were generated by LA-PCR kit Ver. 2 (Takara, Shiga, Japan) using the 14 kb minigene GLUT4 construct with a "tag" as a template, Takara LA *Taq* polymerase, and the following primers: 5′ primer, 5′-CGCATC-GGATCC(*Bam*HI)-TTGCCCTCCCCCGCCTGGGACA-3′; 3′ primer, 5′-CGCATC-GGATCC(*Bam*HI)-CTGCAGGTCAACGGATCAGTGG-3′. The PCR products were digested with *Bam*HI and subcloned into the *Bam*HI site of pGEM-3ZX [13]. The integrity of the constructs was confirmed by DNA sequencing. The effects of PCR introduced mutations on GLUT4 minigene expression study were explained and discussed in our previous study [12,14]. After large-scale propagations of these plasmids harboring constructs, the plasmids were digested by *Sal*I and the linearized minigene constructs were isolated by agarose gel electrophoresis, followed by electroelution. These minigene constructs were further purified by NACS cartridge (Gibco-BRL, Tokyo, Japan) and used for microinjection into the pronucleus of fertilized mouse embryos at the Chrysalis DNX, Inc. Transgenic Animal Sciences (Princeton, NJ) and Japan SLC (Hamamatsu, Japan).

Transgenic mice. Transgenic mice harboring GLUT4 minigene were identified by Southern blot [15] using 281 bp of a "tag" as described previously [13]. The 281-bp tag inserted into the 3′-untranslated region of the gene allowed transcript detection without disrupting translation of minigene mRNA. RNase protection analysis utilized an antisense RNA probe that generates protected fragments of 433 and 399 bp corresponding to the minigene GLUT4 transcript and those of 182 bp corresponding to the endogenous GLUT4 transcript [12]. These transcripts were quantified with a BAS 2000 image analyzer (Fuji Film, Tokyo, Japan). Heterozygous transgenic mice were used for the following studies at 10–20 weeks of age.

High-fat diet. The composition of the diets was prepared as described previously [16]. Mice were fed ad libitum either a high-carbohydrate diet containing 4% safflower oil, 23.7% casein, 0.3% L-cystine, 10% sucrose, 50% starch, 1% vitamin mixture, 7% mineral mixture, and 4% cellulose powder or a high-fat diet containing 32% safflower oil, 33.1% casein, 0.3% L-cystine, 17.6% sucrose, 1.4% vitamin mixture, 9.8% mineral mixture, and 5.6% cellulose powder. Preliminary feeding trials were conducted, and the composition of the diets was adjusted so that the daily intake of calories and the amount of dietary components, except fat and carbohydrate, were nearly identical. The diets were continued for 4 months, after which the animals were sacrificed and total RNA was isolated. The mice were cared in accordance with "Principles of Laboratory Animal Care" (NIH publication No. 85-23, revised 1985:http://grants1.nih.gov/grants/onlaw/references/phspol.htm) and our institutional guidelines.

Preparation of nuclear extracts. C57BL/6J male mice were obtained from Tokyo Laboratory Animal Science (Tokyo, Japan) at 7 weeks of age. Nuclear extract was prepared as described by Hahn and Covault with modifications [17]. Three grams of WAT, brown adipose tissue (BAT) or skeletal muscle (gastrocnemius) was homogenized in 25 ml of Buffer A (0.3 M sucrose, 60 mM KCl, 0.15 mM spermine, 0.5 mM spermidine, 0.5 mM EGTA, 2 mM EDTA, 14 mM of 2-mercaptoethanol, 10 mg/ml BSA, and 15 mM Hepes, pH 7.5) using a Polytron (12-mm shaft, Kinematica AG, Littau, Switzerland) for 15 s each at 70–80% of maximum power on ice. The homogenate was centrifuged in a Hitachi RPR 20-2 rotor for 5 min at 3000 rpm and the pellet was re-homogenized using the Polytron in 20 ml of Buffer B (as Buffer A, but with 0.1 mM EGTA and 0.1 mM EDTA) for 15 s at 70–80% of maximum power on ice. Triton X-100 was added to a final concentration of 0.5% (v/v) and the sample was hand-homogenized using a Teflon-pestle glass homogenizer. The resulting homogenate was filtered through 100 μm-diameter nylon mesh. Percoll (Amersham Bioscience, Tokyo, Japan) was added to the filtrate to a final concentration of 27% (v/v) and the mixture was centrifuged in a RPR 20-2 rotor at 15,000 rpm (27,000*g*) for 15 min. The nuclear layer near the bottom of the centrifuge tube was removed with a pasteur pipette, diluted with 10 vol. of Buffer B, layered on a 1-ml pad of nuclei storage buffer (50% glycerol, 75 mM NaCl, 5 mM magnesium acetate, 0.85 mM DTT, 0.125 mM PMSF, and 20 mM Tris–HCl, pH 7.9), and centrifuged in a RPR 20-2 rotor at 3000 rpm (1000*g*) for 10 min. The nuclear pellet was removed from the bottom of the tube, transferred to 1.5-ml microtube, and centrifuged at 1000*g* for 10 min. After removing the supernatant carefully, the nuclear pellet was added to NUN buffer (1.1 M urea, 0.33 M NaCl, 1.1% NP-40, 17.5 mM Hepes, pH 7.6, and 1 mM DTT) and vigorously vortexed, placed on ice for 30 min, and then centrifuged at 17,010*g* (15,000 rpm) for 10 min in 4 °C. The supernatant was collected as a nuclear extract. The protein concentration of the nuclear extracts was determined by BCA method (Micro BCA kit, Pierce, Rockford, IL). Nuclear extract was quick-frozen in liquid nitrogen and then stored at −80 °C.

Gel mobility shift assay. A double-stranded oligonucleotide probe corresponding to −556 to −527 or −608 to −582 (oligo-1) and −531 to −502 or −586 to −554 (oligo-2) of the 5′-flanking region of the murine or human GLUT4 gene was synthesized, respectively (Fig. 3).

The sequences of synthetic mutated oligo-1 are shown in Fig. 4. All of the oligos were labeled with [γ-^{32}P]ATP (NEN) by T4 polynucleotide kinase (Takara, Shiga, Japan). Ten micrograms of nuclear protein in 4 μl of NUN buffer or 4 μl of in vitro TNT product was added to 21 μl of reaction mixture (9% glycerol, 10 mM NaCl, and 20 mM Tris–HCl, pH 7.4) containing radiolabeled probe (50,000 cpm), 0.5 μg poly(dI–dC)(dI–dC) (Amersham Biochem, Tokyo, Japan). The binding reaction was incubated on ice for 30 min and then separated by electrophoresis on a 4.6% polyacrylamide gel in 0.5× TBE buffer.

UV cross-linking assay. A modified oligonucleotide was prepared substituting bromodeoxyuridine for thymidine in the oligo-1-wt or the oligo-1-M3 in Fig. 4A. The DNA–protein complex was allowed to form under the same conditions used in gel mobility shift assay as described above, except that after incubation, the binding reaction was cross-linked by exposure to UV light at 312 nm for 25 min. The binding reactions were then subjected to a 7.5% SDS–PAGE to resolve the cross-linked DNA–protein complex.

Results

Localization of a sequence element for adipose tissue specific expression (ASE) of GLUT4

RNase protection analysis was made to examine expression patterns of minigene and endogenous GLUT4 from −506 GLUT4 transgenic mice in various tissues. Since expression of GLUT4 minigene was affected by the genomic integration site and construct copy number in mouse genome, two independent founder lines, line −506a and line −506d, were analyzed. The autoradiogram (Fig. 1) and its relative expression levels (Fig. 2) of various tissues from male and female mice of two independent founder lines are shown. In male and female mice from both lines of mice, the GLUT4 minigene was expressed at substantial levels in skeletal muscles (gastrocnemius and quadriceps) and heart, but was not expressed or very weakly expressed in WAT and BAT, while endogenous GLUT4 was expressed in all these insulin sensitive tissues. The line −506d mice expressed a much larger amount of GLUT4 minigene mRNA in skeletal muscles and heart than those in line −506a transgenic mice. These results indicated that the −506 GLUT4 minigene construct does not contain the nucleotide sequences required for GLUT4 expression in WAT and BAT. Since in our previous study GLUT4 minigene expressed in WAT and BAT in −551 GLUT4 transgenic mice [14], ASE is located within 45 bp between bases −551 and −506 of the GLUT4 gene.

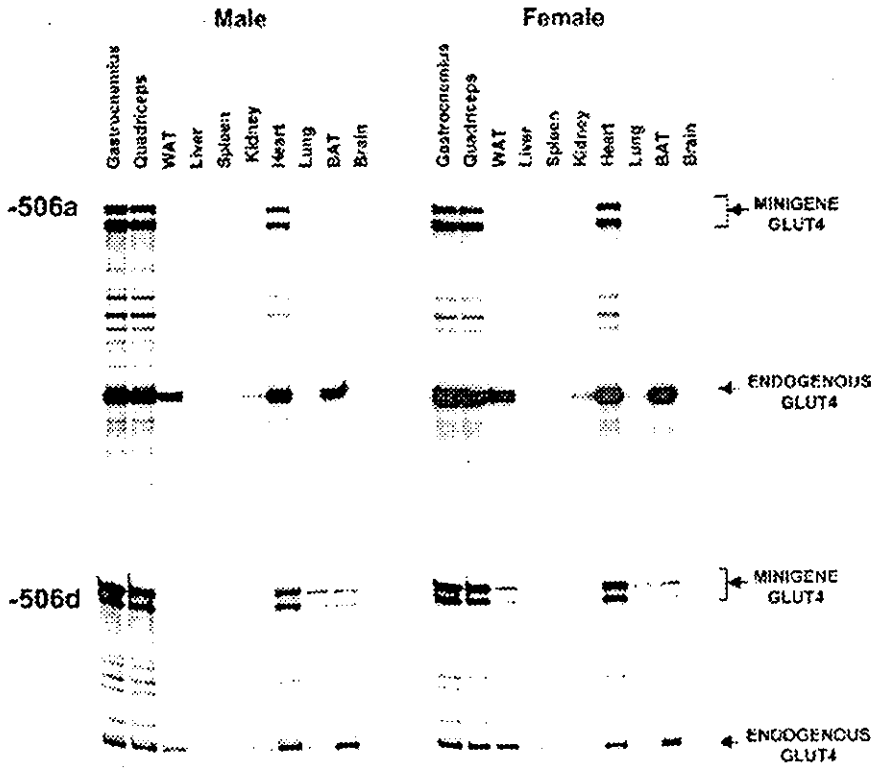

Fig. 1. Expression of minigene and endogenous GLUT4 mRNAs in transgenic mice harboring −506 GLUT4 minigene. Total RNA isolated from the indicated tissues of male and female heterozygous transgenic mice was subjected to RNase protection analysis as described under "Materials and methods." Results from two independent mice lines (a and d) are shown. The 433- and 399-bp protected fragments correspond to minigene GLUT4 transcript and the 182-bp protected fragment corresponds to endogenous GLUT4 transcript (arrows). Several bands observed between 399 and 182 bp appear to be degraded fragments of the minigene-protected fragment. Gels were exposed to X-ray film at −80 °C for 3–8 h. Quantification of minigene and endogenous GLUT4 transcripts is presented in Fig. 2.

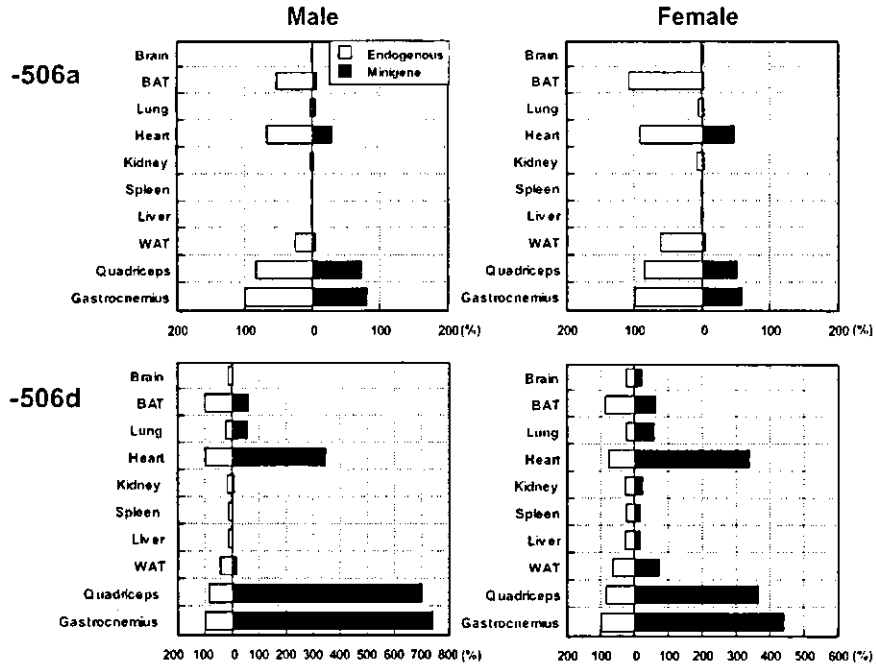

Fig. 2. Tissue-specific expression of GLUT4 mRNAs derived from minigene and endogenous GLUT4 in male and female heterozygous −506 GLUT4 transgenic mice. Total RNA isolated from the indicated tissues of male and female heterozygous transgenic mice was subjected to RNase protection analysis as described under "Materials and methods." The size of the open and solid boxes indicates radioactivity levels of endogenous and minigene GLUT4 protected fragments shown in Fig. 1, respectively. The expression levels of the minigene and endogenous GLUT4 transcripts were expressed as a percentage of that of endogenous GLUT4 transcript from gastrocnemius. Since minigene GLUT4 protected fragments (433 and 399 bp) have radioactivity about 2-fold greater than that of endogenous GLUT4 protected fragments (182 bp), the actual mRNA level of minigene GLUT4 was half of its radioactivity in comparison with endogenous GLUT4.

Identification of nuclear protein–DNA complexes binding to ASE of GLUT4 gene

The sequence of 45 bp between −551 and −506 of the mouse GLUT4 gene is presented in Fig. 3A. As reference, a sequence of human GLUT4 corresponding to this mouse sequence is also presented. The mice and human sequences are highly conserved; the mice and human genes are 82% identical between bases −551 and −506 of the mouse GLUT4 gene. To examine the existence of nuclear binding protein(s) to these sequences in WAT, BAT, and skeletal muscle nuclear extracts, using two synthetic double-stranded oligonucleotide probes (oligos-1 and -2) that covered 45 bp between −551 and −506 of the mouse GLUT4 gene and its corresponding human GLUT4 gene, gel shift analysis was performed (Fig. 3B). As for the oligo-1 probe, one major protein–DNA complex was identified in WAT nuclear extract (indicated as an arrow in Fig. 3B). This protein–DNA complex was formed also in the nuclear extracts from BAT and skeletal muscle, and was much stronger when human oligo-1 probe was used than when mouse oligo-1 probe was used. In BAT and skeletal muscle nuclear extracts, the other slower migrating protein–DNA complex was observed, while in WAT nuclear extract, this complex was not observed. In oligo-2, no appreciable binding protein was found in WAT nuclear extract, but several protein–DNA complexes were identified in BAT and skeletal muscle nuclear extracts. Since the major protein–DNA complex was observed in both mouse and human oligo-1 in WAT nuclear extract, in the following study we focused on this protein, tentatively named protein X.

Identification of nucleotide sequence responsible for binding the protein X

To further define the sequence necessary for binding to the nuclear protein, mutant oligonucleotides were tested for their ability to bind to WAT and BAT nuclear extracts (Fig. 4). Mutant 1 (M1), with five base changes in the 5′ end of the oligonucleotide, could bind the protein X. Mutant 2 (M2), with five base changes next to M1 oliginucleotides, could partially bind the protein X. Mutants 3 and 4, with five base changes in the middle of the oliginucleotides, could not bind the protein X. Mutants 5 and 6, with five base changes in the 3′ end of the oliginucleotides, could bind the protein X. These binding profiles are observed in both WAT and BAT nuclear extracts. These data indicated that a 15 base sequence -TCCTCGTGGGAAGCG-, which was located between bases −551 and −537 in the

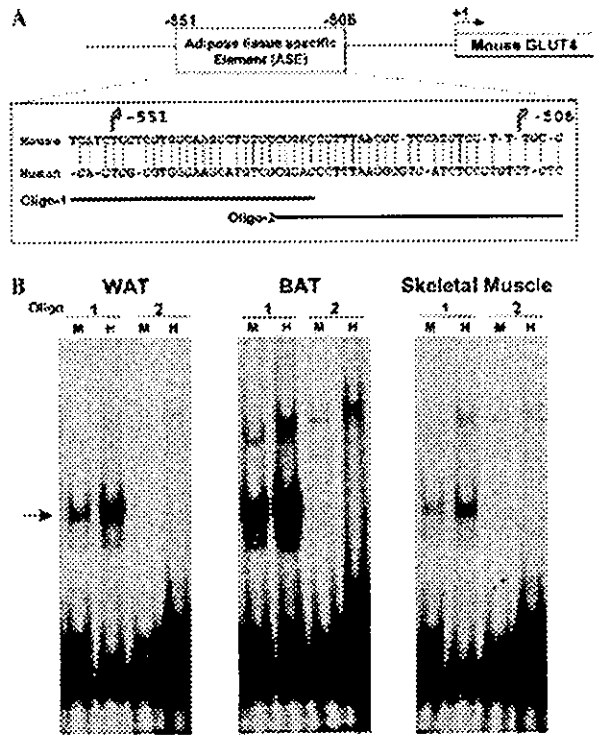

Fig. 3. Binding of nuclear proteins from WAT, BAT, and skeletal muscle to the oligo-1 and oligo-2. Shown in (A) are nucleotide sequence of 45 bp between −551 and −506 of the mouse GLUT4 nucleotide sequence and its corresponding human GLUT4 gene. The oligo-1 and oligo-2 indicated the synthetic double-stranded oligonucleotide probes used for gel shift analysis. In (B), 10 μg of nuclear extracts from WAT, BAT, and skeletal muscle was incubated with [γ-^{32}P]ATP labeled double-stranded mouse (M) or human (H) oligonucleotides, oligo-1 and oligo-2, for 30 min on ice. The protein–DNA mixtures were resolved on an 8% polyacrylamide gel. Gels were exposed to X-ray film at −80 °C for 12 h. Arrow indicates specific protein–DNA complexes.

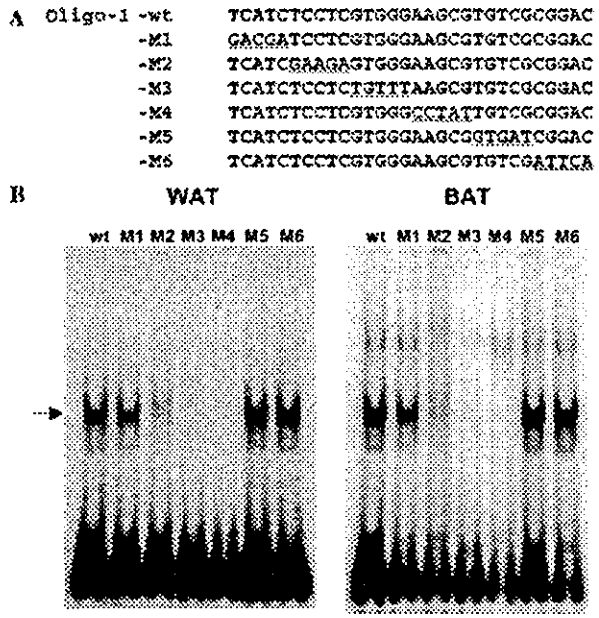

Fig. 4. Binding of WAT and BAT nuclear proteins to the mutated oligo-1s. Shown in (A) are the sequences of wild type mouse oligo-1, mutated M1, M2, M3, M4, M5, and M6 oligo-1s. In (B), 10 μg of nuclear extracts from WAT and BAT was incubated with these [γ-^{32}P]ATP labeled double-stranded oligonucleotides for 30 min on ice. The protein–DNA mixtures were resolved on an 8% polyacrylamide gel. Gels were exposed to X-ray film at −80 °C for 12 h. Arrow indicates specific protein–DNA complexes.

mouse GLUT4 gene, was responsible for binding the protein X.

Molecular size(s) of the protein X

To estimate the molecular size(s) of the protein X, we performed an experiment in which the DNA–protein complex was UV cross-linked using a radiolabeled double-stranded oligonucleotide corresponding to oligo-1 (Fig. 5). A major band, binding specifically to the wild-type oligonucleotide, migrated at a position corresponding to approximately 80-kDa. A less abundant band was observed to migrate at the 250-kDa marker.

Localization of high-fat-responsive element(s) in mouse GLUT4 gene

In our previous study, high-fat-responsive element (HFRE) is located within 558 bp between −1001 and −442 relative to transcription initiation [12]. To examine whether ASE were also responsible for high-fat diet-induced down-regulation of GLUT4, −701c, −551b, and −551c GLUT4 transgenic mice were fed either high-carbohydrate diet or high-fat diet for 4 months. Tissue specific GLUT4 expression profiles in these transgenic mice have been described in our previous study [14]. Since −506 GLUT4 transgenic mice did not express GLUT4 in adipose tissues (Figs. 1 and 2), this transgenic mice line was not examined. In WAT, the high-fat diet feeding caused 56% decrease in the endogenous GLUT4 mRNA in the −701c and −551b transgenic mice (Fig. 6). Paralleled with the decreased endogenous GLUT4 mRNA, the −701 GLUT4 transgenic mice showed 55% decreases of minigene GLUT4 mRNA levels in WAT. However, the −551b GLUT4 transgenic mice failed to decrease minigene GLUT4 mRNA. In addition, although endogenous GLUT4 mRNA was decreased by 29% in another independent −551c transgenic mice, only 9% of decreases of minigene mRNA was observed. Similar to −701c transgenic mice, in −3238b, −2001c, −1001a transgenic mice, high-fat diet down-regulated both minigene, and endogenous GLUT4 mRNAs as observed in the previous study (Fig. 6B) [12]. These results indicated that HFRE is located within 150 bp between −701 and −551 and differed from the ASE.

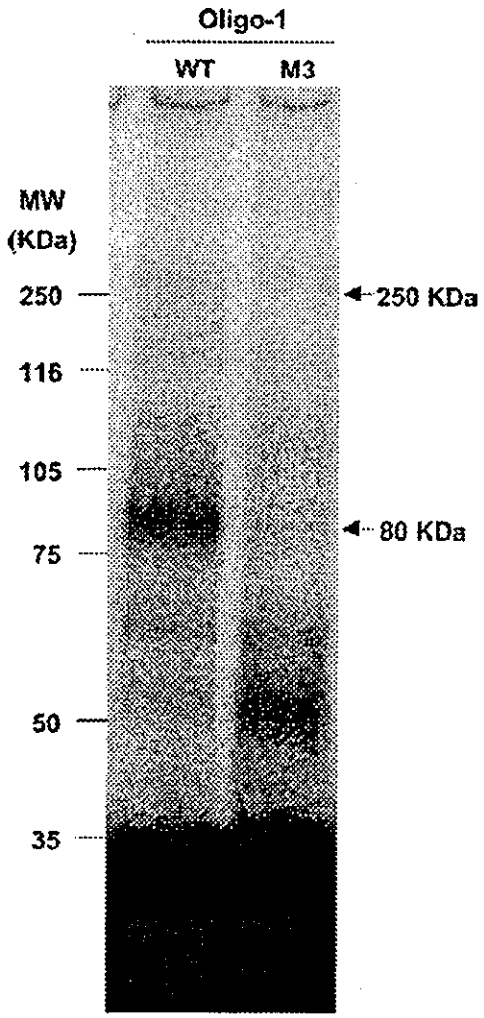

Fig. 5. UV cross-linking of nuclear proteins to oligo-1. Ten micrograms of nuclear extract from BAT was incubated with [γ-^{32}P]ATP labeled double-stranded oligo-1-wt or oligo-1-M3 in Fig. 4A for 30 min on ice. The binding reaction was exposed to UV light. The protein-DNA mixtures were resolved on a 7.5% SDS-PAGE. Gels were exposed to X-ray film at −80 °C for 12 h. Arrows indicate specific protein–DNA complexes.

Discussion

In this study, using 5′-deletion analysis of the mouse GLUT4 minigene in transgenic mice, we have located the *cis*-element(s) for the adipose tissue specific GLUT4 expression (ASE) and the *cis*-element(s) for the down-regulation of GLUT4 by high-fat diet (HFRE). These *cis*-elements were distinct; ASE located within 45 bp were located between bases −551 and −506, while HFRE located within 150 bp were located between bases −701 and −551. Furthermore, by gel shift analysis, we found a nuclear protein that bound to 15 bp located between bases −551 and −537 (-TCCTCGTGGGAAGCG-). This protein (protein X) had a molecular size, 80-kDa, and might be an unidentified protein, since there is no transcription factor binding motif(s) in the vertebrate database that matched completely to this sequence by a computer program, TFSEARCH (http://molsun1.cbrc.aist.go.jp/research/db/TFSEARCHJ.html).

Fully differentiated adipocytes express proteins involved in basic functions of adipocyte including insulin-sensitive glucose uptake [18]. Transcription of the genes for these proteins is regulated by at least two families of transcription factors, CCAAT/enhancer-binding proteins (C/EBPs) and peroxisome proliferator-activated receptors (PPARs) [19]. Experimental evidences show that C/EBPα is required for transcription of GLUT4 gene during adipogenesis [20,21]. However, although putative C/EBP binding site was found in GLUT4 5′-flanking sequence [22], the sequence within 45 bp located between bases −551 and −506 of mouse GLUT4 gene did not contain this binding site. PPAR-responsive element (PPRE) has not been found in GLUT4 5′-flanking region. The results suggest that the adipose tissue expression of GLUT4 in vivo requires different or additional transcription factor(s) and mechanism(s). In the present study, we showed the 45 bp DNA sequence that is required for GLUT4 expression in adipose tissues and the presence of nuclear protein (protein X) that bound to this sequence. It suggested that the protein X was possibly a critical transcription factor for the expression of GLUT4 in adipose tissues. The protein X was expressed not only in adipose tissues but also in skeletal muscles, suggesting that adipose tissue specific activation of this transcription factor, possibly by the phosphorylation/dephosphorylation or the interaction with other transcription factor(s) and co-factor(s), might be involved in the increased GLUT4 expression.

In transgenic mice using 5′-deletion and mutation analysis of the human GLUT4-CAT (hG4-CAT) reporter gene, Olson's group revealed that both a MEF2 binding site (−473 to −464 corresponding to mouse −437 to −428) and Domain I (−772 to −712 corresponding to mouse −714 to −654) were necessary for all insulin-sensitive tissue (WAT, BAT, heart, and skeletal muscles) specific expression of GLUT4 [23–25]. However, the protein X binding site located between Domain I to MEF2 binding site. As for ASE, the results from the human GLUT4-CAT reporter gene study were not in good agreement with our results from mouse GLUT4 minigene. One of the possible reasons to explain this discrepancy is that the other important *cis*-element(s) for GLUT4 expression may be located in intronic or 3′-untranslated regions of the GLUT4 gene. Indeed, in our previous study, the −423 GLUT4 minigene that lacks the MEF2 binding site could express substantial levels of minigene GLUT4 mRNA in skeletal muscles, suggesting an existence of other important transcription factors [14]. These other important transcription factors may interact with MEF2 and protein X for the regulation of GLUT4.

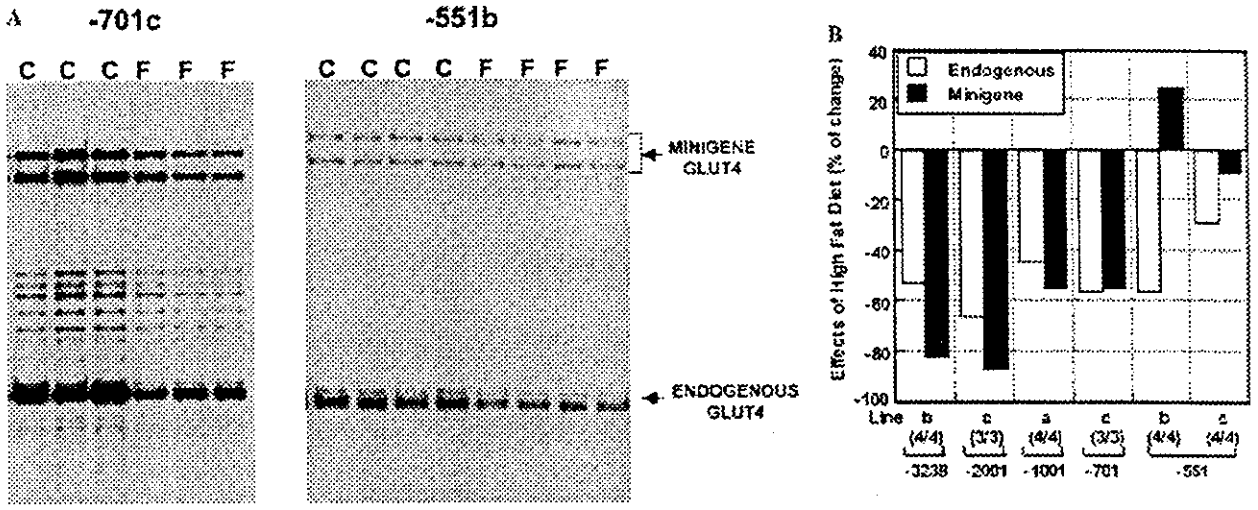

Fig. 6. Regulation of minigene and endogenous GLUT4 mRNA in white adipose tissues from female high-fat diet fed mice. Heterozygous female transgenic mice of −3238b, −2001c, −1001a, −701c, −551b, and −551c described in the previous study [12,14] were divided into two groups, one subjected to high-carbohydrate feeding protocol (C) and the other to high-fat feeding protocol (F). Total RNAs isolated from parametrial WAT were subjected to RNase protection assays. In (A), autoradiogram of −701c and −551b transgenic mice is shown. The 433- and 399-bp protected fragments correspond to minigene GLUT4 transcript and the 182-bp protected fragment corresponds to endogenous GLUT4 transcript. Gels were exposed to X-ray film at −80 °C for 4–12 h. In (B), the minigene and endogenous GLUT4 expression levels in WAT were quantified by image analyzer and expressed by relative percent to endogenous GLUT4 transcript in WAT from high-carbohydrate fed mice. The high-fat feeding effects were expressed as a percent decrease of GLUT4 mRNA in high-fat diet fed mice relative to those in high-carbohydrate diet fed mice. Each data point is the mean ± standard error of the mean of 3–4 mice. The number of mice studied (high-carbohydrate feeding/high-fat feeding) is shown in parentheses.

The homology of human and mice GLUT4 sequence in 45 bp between mouse −551 and −506 was 82%, suggesting a physiological importance in this sequence. In fact, the comparison between human (GenBank Accession No. M61126) and mouse GLUT4 gene 5′ flanking region (GenBank Accession No. M29660) by BLAST2 sequences program (http://www.ncbi.nlm.nih.gov/blast/bl2seq/bl2.html), that produces the alignment of two given sequences using BLAST engine for local alignment, showed 85% of identity was found between human −602 to −457 and mouse −547 to −404, and 96% of that was found between human −124 to −66 and mouse −130 to −72. Thus, these common sequences might be physiologically important, since a critical *cis*-element is usually conserved among the species.

Down-regulation of GLUT4 by high-fat diet was mediated by 150 bp between bases −701 and −551 in the mouse gene promoter. This sequence includes NF-1 and Olf-1/Early B cell factor binding sites, which mediate insulin and cyclic AMP-induced down-regulation of GLUT4 in 3T3-L1 adipocytes [26–29] and Domain I [23]. Thus, these sequences may be responsible for the regulation of GLUT4 by metabolic changes. Recently, just downstream of MEF2 binding site, liver X receptor (LXR) binding site was found, which was suggested to work as an enhancer of GLUT4 expression in adipose tissues using 3T3-L1 adipocytes [30]. However, LXR per se is not necessary for adipocyte GLUT4 expression but may regulate GLUT4 expression with other elements, such as ASE, NF-1 binding site, Domain I, and MEF2.

To clarify these complex, regulatory mechanism(s) of GLUT4 expression in adipose tissues, further studies including the cloning of protein X and mutational analysis of ASE and HFRE in transgenic mice are needed.

Acknowledgments

We are indebted to Dr. D.W. Cooke at Johns Hopkins University for his helpful discussion. This work was supported in part by a Grant-in-Aid for Scientific Research KAKENHI 14770030 (to S.M.) from the Japanese Ministry of Education, Culture, Sports, Science and Technology (MEXT, Tokyo), and by research grants from the Japanese Ministry of Health, Labor and Welfare (Tokyo), by a grant from the Promotion of Fundamental Studies in Health Sciences of Organization for Pharmaceutical Safety and Research (OPSR).

References

[1] J.M. Ren, B.A. Marshall, E.A. Gulve, J. Gao, D.W. Johnson, J.O. Holloszy, M. Mueckler, Evidence from transgenic mice that glucose transport is rate-limiting for glycogen deposition and glycolysis in skeletal muscle, J. Biol. Chem. 268 (1993) 16113–16115.

[2] D.L. Rothman, R.G. Shulman, G.I. Shulman, ^{31}P nuclear magnetic resonance measurements of muscle glucose-6-phosphate. Evidence for reduced insulin-dependent muscle glucose transport or phosphorylation activity in non-insulin-dependent diabetes mellitus, J. Clin. Invest. 89 (1992) 1069–1075.

[3] T.B. Price, G. Perseghin, A. Duleba, W. Chen, J. Chase, D.L. Rothman, R.G. Shulman, G.I. Shulman, NMR studies of muscle glycogen synthesis in insulin-resistant offspring of parents with non-insulin-dependent diabetes mellitus immediately after

glycogen-depleting exercise, Proc. Natl. Acad. Sci. USA 93 (1996) 5329–5334.
[4] B.B. Kahn, Lilly lecture 1995. Glucose transport: pivotal step in insulin action, Diabetes 45 (1996) 1644–1654.
[5] M. Okamoto, M. Okamoto, S. Kono, G. Inoue, T. Hayashi, A. Kosaki, I. Maeda, M. Kubota, H. Kuzuya, H. Imura, Effects of a high-fat diet on insulin receptor kinase and the glucose transporter in rats, J. Nutr. Biochem. 3 (1992) 241–250.
[6] O. Ezaki, N. Fukuda, H. Itakura, Role of two types of glucose transporters in enlarged adipocytes from aged obese rats, Diabetes 39 (1990) 1543–1549.
[7] P.R. Shepherd, L. Gnudi, E. Tozzo, H. Yang, F. Leach, B.B. Kahn, Adipose cell hyperplasia and enhanced glucose disposal in transgenic mice overexpressing GLUT4 selectively in adipose tissue, J. Biol. Chem. 268 (1993) 22243–22246.
[8] E.D. Abel, O. Peroni, J.K. Kim, Y.B. Kim, O. Boss, E. Hadro, T. Minnemann, G.I. Shulman, B.B. Kahn, Adipose-selective targeting of the GLUT4 gene impairs insulin action in muscle and liver, Nature 409 (2001) 729–733.
[9] O. Pedersen, C.R. Kahn, J.S. Flier, B.B. Kahn, High fat feeding causes insulin resistance and a marked decrease in the expression of glucose transporters (Glut 4) in fat cells of rats, Endocrinology 129 (1991) 771–777.
[10] W.T. Garvey, L. Maianu, T.P. Huecksteadt, M.J. Birnbaum, J.M. Molina, T.P. Ciaraldi, Pretranslational suppression of a glucose transporter protein causes insulin resistance in adipocytes from patients with non-insulin-dependent diabetes mellitus and obesity, J. Clin. Invest. 87 (1991) 1072–1081.
[11] W.T. Garvey, L. Maianu, J.A. Hancock, A.M. Golichowski, A. Baron, Gene expression of GLUT4 in skeletal muscle from insulin-resistant patients with obesity, IGT, GDM, and NIDDM, Diabetes 41 (1992) 465–475.
[12] N. Tsunoda, D.W. Cooke, S. Ikemoto, K. Maruyama, M. Takahashi, M.D. Lane, O. Ezaki, Regulated expression of 5′-deleted mouse GLUT4 minigenes in transgenic mice: effects of exercise training and high-fat diet, Biochem. Biophys. Res. Commun. 239 (1997) 503–509.
[13] O. Ezaki, J.R. Flores-Riveros, K.H. Kaestner, J. Gearhart, M.D. Lane, Regulated expression of an insulin-responsive glucose transporter (GLUT4) minigene in 3T3-L1 adipocytes and transgenic mice, Proc. Natl. Acad. Sci. USA 90 (1993) 3348–3352.
[14] N. Tsunoda, K. Maruyama, D.W. Cooke, M.D. Lane, O. Ezaki, Localization of exercise- and denervation-responsive elements in the mouse GLUT4 gene, Biochem. Biophys. Res. Commun. 267 (2000) 744–751.
[15] E.M. Southern, Detection of specific sequences among DNA fragments separated by gel electrophoresis, J. Mol. Biol. 98 (1975) 503–517.
[16] S. Ikemoto, K.S. Thompson, M. Takahashi, H. Itakura, M.D. Lane, O. Ezaki, High fat diet-induced hyperglycemia: prevention by low level expression of a glucose transporter (GLUT4) minigene in transgenic mice, Proc. Natl. Acad. Sci. USA 92 (1995) 3096–3099.
[17] C.G. Hahn, J. Covault, Isolation of transcriptionally active nuclei from striated muscle using Percoll density gradients, Anal. Biochem. 190 (1990) 193–197.
[18] P. Cornelius, O.A. MacDougald, M.D. Lane, Regulation of adipocyte development, Annu. Rev. Nutr. 14 (1994) 99–129.
[19] E.D. Rosen, B.M. Spiegelman, Molecular regulation of adipogenesis, Annu. Rev. Cell. Dev. Biol. 16 (2000) 145–171.
[20] F-T. Lin, M.D. Lane, Antisense CCAAT/enhancer-binding protein RNA suppresses coordinate gene expression and triglyceride accumulation during differentiation of 3T3-L1 preadipocytes, Genes Dev. 6 (1992) 533–544.
[21] A.K. El-Jack, J.K. Hamm, P.F. Pilch, S.R. Farmer, Reconstitution of insulin-sensitive glucose transport in fibroblasts requires expression of both PPARγ and C/EBPα, J. Biol. Chem. 274 (1999) 7946–7951.
[22] O. Ezaki, Regulatory elements in the insulin-responsive glucose transporter (GLUT4) gene, Biochem. Biophys. Res. Commun. 241 (1997) 1–6.
[23] K.M. Oshel, J.B. Knight, K.T. Cao, M.V. Thai, A.L. Olson, Identification of a 30-base pair regulatory element and novel DNA binding protein that regulates the human GLUT4 promoter in transgenic mice, J. Biol. Chem. 275 (2000) 23666–23673.
[24] M.V. Thai, S. Guruswamy, K.T. Cao, J.E. Pessin, A.L. Olson, Myocyte enhancer factor 2 (MEF2)-binding site is required for GLUT4 gene expression in transgenic mice. Regulation of MEF2 DNA binding activity in insulin-deficient diabetes, J. Biol. Chem. 273 (1998) 14285–14292.
[25] A.L. Olson, J.E. Pessin, Transcriptional regulation of the human GLUT4 gene promoter in diabetic transgenic mice, J. Biol. Chem. 270 (1995) 23491–23495.
[26] D.W. Cooke, M.D. Lane, A sequence element in the GLUT4 gene that mediates repression by insulin, J. Biol. Chem. 273 (1998) 6210–6217.
[27] D.W. Cooke, M.D. Lane, The transcription factor nuclear factor I mediates repression of the GLUT4 promoter by insulin, J. Biol. Chem. 274 (1999) 12917–12924.
[28] D.W. Cooke, M.D. Lane, Transcription factor NF1 mediates repression of the GLUT4 promoter by cyclic-AMP, Biochem. Biophys. Res. Commun. 260 (1999) 600–604.
[29] P. Dowell, D.W. Cooke, Olf-1/early B cell factor is a regulator of glut4 gene expression in 3T3-L1 adipocytes, J. Biol. Chem. 277 (2002) 1712–1718.
[30] B.A. Laffitte, L.C. Chao, J. Li, R. Walczak, S. Hummasti, S.B. Joseph, A. Castrillo, D.C. Wilpitz, D.J. Mangelsdorf, J.L. Collins, E. Saez, P. Tontonoz, Activation of liver X receptor improves glucose tolerance through coordinate regulation of glucose metabolism in liver and adipose tissue, Proc. Natl. Acad. Sci. USA 100 (2003) 5419–5424.

Available online at www.sciencedirect.com
SCIENCE DIRECT
Neuroscience Research 45 (2003) 285–296
Neuroscience Research
www.elsevier.com/locate/neures

Antisense in vivo knockdown of synaptotagmin I and synapsin I by HVJ-liposome mediated gene transfer modulates ischemic injury of hippocampus in opposing ways

Miwa Iwakuma [a,b,*], Takeshi Anzai [c,d], Shizuka Kobayashi [a,b], Masanori Ogata [a], Yasufumi Kaneda [e], Kousaku Ohno [f], Makoto Saji [a,c]

[a] Department of Physiology, School of Allied Health Sciences, Kitasato University, Sagamihara, Kanagawa 228-8555, Japan
[b] Department of Neurobiology, School of Life Science, Faculty of Medicine, Tottori University, Yonago, Tottori 683-8503, Japan
[c] Division of Brain Science, Graduate School of Medical Science, Kitasato University, Sagamihara, Kanagawa 228-8555, Japan
[d] Department of Anesthesiology, School of Medicine, Kitasato University, Sagamihara, Kanagawa 228-8555, Japan
[e] Division of Gene Therapy Science, Graduate School of Medicine, Osaka University, Suita, Osaka 565-0871, Japan
[f] Department of Child Neurology, Institute of Neurological Sciences, Faculty of Medicine, Tottori University, Yonago, Tottori 683-8503, Japan

Received 18 September 2002; accepted 13 November 2002

Abstract

Neurotransmitter release during and after ischemic event is thought to be involved in excitotoxicity as a pathogenesis for the ischemic brain damage, which is mediated by excessive activation of glutamate receptors and attendant calcium overload. To ascertain the role of transmitter release from nerve terminals in promoting the ischemic neurodegeneration, we delivered antisense oligodeoxynucleotides (ODNs) to synaptotagmin I or synapsin I into the rat brain by using HVJ-liposome gene transfer technique. The antisense ODNs were injected into the lateralventricle in rats 4 days prior to transient forebrain ischemia of 20 min. With a single antisense treatment, long-lasting downregulation of the transmitter release relating protein levels at overall synaptic terminals was achieved. The antisense in vivo knockdown of synaptotagmin I prevented almost completely the ischemic damage of hippocampal CA1 neurons, while the in vivo knockdown of synapsin I markedly promoted the ischemic damage of CA1 pyramidal neurons and extended the injury to relatively resistant CA2/CA3 region. The modulation of ischemic hippocampal damage by the in vivo knockdown of synaptotagmin I or synapsin I suggests that transmitter release from terminals plays an important role in the evolution of ischemic brain damage and therefore the transmitter release strategy by the use of antisense ODNs–HVJ-liposome complex is reliable for neuroprotective therapies.

Keywords: Antisense oligodeoxynucleotides; Ischemic neurodegeneration; Hippocampus; Synaptotagmin I; Synapsin I; HVJ-liposome mediated gene transfer method

1. Introduction

The synaptic release of excitatory amino acid glutamate following an ischemic insult is thought to be an important factor in the development of neuronal death. Surgical removal of glutamatergic afferent fibers to the hippocampus prevented the ischemia-induced damage of CA1 pyramidal neurons in the hippocampus (Wieloch et al., 1985; Onodera et al., 1986; Jorgensen et al., 1987; Buchan and Pulsinelli, 1990). Furthermore, AMPA receptor antagonist but not NMDA receptor antagonist markedly attenuated the ischemic cell death of CA1 pyramidal neurons, even when administrated hours after an ischemic insult (Sheardown et al., 1990, Nellgard and Wieloch, 1992; Sheardown et al., 1993). The neuroprotection afforded by surgical transection of glutamate containing afferents to the CA1 neurons and postischemic pharmacological blockade of glutamate receptors strongly supports the notion that a major determinant of the glutamate receptor-mediated excito-

* Corresponding author. Tel./fax: +81-427-78-8153.
E-mail address: mi5603@ahs.kitasato-u.ac.jp (M. Iwakuma).

0168-0102/02/$ - see front matter
PII: S0168-0102(02)00233-X

toxicity in ischemic brain injury may be excitatory transmitter glutamate released from synaptic terminals in a stimulus-dependent manner after ischemic insult (Benveniste et al., 1989). However, it is not fully understood whether the synaptic release of glutamate at nerve terminals is most responsible for the excitotoxic intracellular processes leading to cell death of neurons.

Wahlestedt et al. have demonstrated that antisense-induced in vivo knockdown of NMDA receptor subunit NR1 markedly attenuated ischemic brain damege (Wahlestedt et al., 1993). However, recent studies have shown that the major problems with antagonists of glutamate receptors are psychomimetic effects, sedation and catatonia (De Keyser et al., 1999), probably due to drug-induced imbalance between dopaminergic and glutamatergic system. Since modulation of presynaptic release would affect all the synapses, an antisense knockdown of transmitter-release relating protein is expected to minimize treatment-induced derangement in the interaction between multiple chemical transmitter systems. Therefore, an antisense in vivo knockdown of transmitter-release relating protein seems to be a promising strategy to develop the effective therapies for ischemic brain injury with the less side-effect.

Among exocytosis-relating proteins that are abundant at nerve terminals, synapsin I as a protein related to synaptic vesicle trafficking is considered to control rates of synaptic vesicle exocytosis by participating in regulation of the vesicle life cycle via dissociation-reassociation cycle of synapsin with vesicle depended on phosphorylation (Hilfiker et al., 1998; Hosaka et al., 1999; Chi et al., 2001; Murthy, 2001). Synaptotagmin I as a major Ca^{2+} sensor is considered to regulate the synaptic vesicle exocytosis by promoting fusion between synaptic vesicle and plasma membrane via the assembly and clustering of SNARE complex (Bommert et al., 1993; Littleton et al., 1993; Nonet et al., 1993; Geppert et al., 1994; Littleton et al., 2001). According to the possible role of these proteins in transmitter release, it has been postulated that both antisense in vivo knockdown of synapsin I and that of synaptotagmin I reduces rates of exocytotic release of transmitter at overall synaptic terminals. To achieve a long-lasting downregulation of synapsin I or synaptotagmin I by a single treatment with the antisense oligodeoxynucleotides (ODNs), we used a novel transfection vector (HVJ-liposome)(Kaneda et al., 1989; Tomita et al., 1992; Morishita et al., 1994).

To test the relevance of the 'transmitter-release strategy' for neuroprotective therapies to regulate ischemic brain injury, we injected the antisense ODNs against synaptotagmin I or synapsin I into the lateralventricle by using HVJ (hemagglutinating virus of Japan)-liposome mediated gene transfer technique prior to transient forebrain ischemia and examined whether the antisense-induced knockdown of synaptotagmin I or synapsin I in the whole brain could regulate ischemia-induced damage of neurons in the hippocampus.

2. Materials and methods

2.1. Preparation of HVJ-liposome containing oligodeoxynucleotides

Detailed preparation of anionic HVJ-liposome containing ODNs (ODNs–HVJ-liposome) has been described elsewhere (Yamada et al., 1996;Saeki and Kaneda, 1998). Briefly, three kinds of lipid (phosphatidylserine, phosphatidylcholine, and cholesterol) dissolved in chloroform (1 mg/ml) were mixed in a weight ratio of 1:4.8:2. Ten milligrams of lipid mixture was transferred into a glass tube and dried as a thin lipid film by rotary evaporator filled with nitrogen gas at 40 °C. The lipid thin film layering on the bottom of a glass tube was hydrated in 200 μl balanced salt solution (BSS: 137 mM NaCl, 5.4 mM KCl, 10 mM Tris–HCl, pH 7.5) containing 100 μg of ODNs (10.6 nmol synapsin I antisense or 7.1 nmol synaptotagmin I antisense) which were dispersed in the aqueous phase at room temperature. The mixture of the hydrated lipid thin film and ODNs was agitated by vortexing for 30 s and then incubated at 37 °C for 30 s. This procedure was repeated 8 times, making fragments of lipid thin film into liposomes in which ODNs were packaged up. The liposome suspension was sonicated for 20 s and vortexed for 30 s. Then 300 μl of BSS was added to the liposomes suspension and incubated at 37 °C for 30 min shaking. The liposome suspension prepared above (500 μl) was mixed with 1 ml suspension of HVJ (more than 10,000 hemagglutinating units), of which RNA genome was inactivated by ultraviolet irradiation (198 mJ/cm^2) just before use. The mixture was incubated at 4 °C for 10 min and at 37 °C for 1 h shaking to facilitate the fusion between inactivated HVJ and liposome. The ODNs–HVJ-liposome complex was loaded onto a discontinuous sucrose gradient and centrifuged at 25,000 rpm at 4 °C for 1.5 h to separate the ODNs–HVJ-liposome complex from free HVJ. The purified ODNs–HVJ-liposomes suspension were adjusted to OD 1.0 (540 nm) with 200–250 μl BSS. Since 10–30% of ODNs (10–30 μg) is available for packing into the liposomes (Kaneda et al., 1989), it is estimated that 1 μl of the purified ODNs–HVJ-liposomes (OD 1.0) is containing about 40–120 ng of ODNs.

2.2. Intraventricular injection of ODNs–HVJ-liposome complex and transient forebrain ischemia

Adult male Wistar rats (weight 220–250 g) were subjected to 20 min of forebrain ischemia by a method previously described (Pulsinelli and Brierley, 1979; Saji

et al., 1994; Kimura and Saji, 1997). Briefly, animals were anesthetized with intraperitoneal sodium pentobarbital (40 mg/kg). The common carotids arteries were exposed and encircled with silastic ligatures, and the vertebral arteries were permanently occluded by electrocautery. After allowing rats to recover from the anesthesia for 24 h, a forebrain ischemia was produced in awaken rats by tightening the carotid ligatures. Rats that lose their righting reflex were classified as ischemic; rats that retained their righting reflex were eliminated from further study. The carotid ligatures were released after 20 min. During the ischemic interval and the reperfusion interval body temperature was maintained at 37 °C by a heating lamp connected to a rectal thermister.

Considering the volume (300–500 μl) of cerebrospinal fluid, we determined that 30 μl of HVJ-liposome containing ODNs is a critical dose for avoiding abnormal increase of inner pressure of the ventricules. Since intraventricular injection of 1 μl of antisense ODNs to synapsin I or that of 1–5 μl of antisense ODNs to synaptotagmin I did not cause significant downregulation of target protein levels in Western blot analysis, we finally determined the optimal dose of HVJ-liposome containing antisense ODNs (10 μl for synapsin I, 30 μl for synaptotagmin I) to induce antisense in vivo knockdown of synapsin I and synaptotagmin I.

Four days prior to the transient forebrain ischemia of 20 min, total 10 μl of HVJ-liposomes containing ODNs (antisense or reversed antisense to synapsin I) or total 30 μl of HVJ-liposome containing ODNs (antisense or reversed antisense to synaptotagmin I) was stereotaxically injected into both side of lateralventricle in the rats. Coordinates for intraventricular injection in mm in respect to ear bar were; (1) AP: 8.1; L: +1.4; D: 4.0, (2) AP: 8.1; L: −1.4; D: 4.0. A glass micropipette (tip size: 30–40 μm; volume: 2.5 μl/cm) made from disposable micropipette (20 μl, Drummond), which was connected to an air pressure system with polyethylen tubing, was used for a single intraventricular injection of the ODNs–HVJ-liposomes.

Sham-operated rats without any prior ODNs-treatment were used as non-treated control animals (NT) in the present study on the ischemic brain damage.

2.3. Antisense oligodeoxynucleotides

Antisense to synapsin I: The phosphorothiolated ODNs (30 mers) corresponding to specific sequences in the 5′-coding region of the synapsin Ia were designed to selectively block the biosynthesis of the synapsin I (Zurmohle et al., 1996) as antisense ODNs to synapsin I (syn-AS: 5′-GTTGAAGGCATTGGTCAGAG ACTGGGATTT-3′). Reversed antisense ODNs (syn-R; 5′-CAACTTCCGTAACCAGTCTCTGACCC-TAAA-3′), in which the bases of the 30-mers syn-AS were reversed, were synthesized for use as a control.

Antisense to synaptotagmin I: The phosphorothiolated ODNs (45 mers) corresponding to specific sequences in the 5′-coding region of synaptotagmin I were designed to selectively block the biosynthesis of synaptotagmin I (Perin et al., 1990) as antisense ODNs to synaptotagmin I (stm-AS: 5′-TGAAGCTATGCTA-GATG CAGTGGTAGGAACGCATTGGCTCCT-GTT-3′). Reversed antisense (stm-R; 5′-ACTTCGA-TACGATCTACGTCACCATCCTTGCGTAACCGA-AGACAA-3′), in which the bases of the 45-mers stm-AS were reversed, was synthesized for use as a control.

Each antisense sequence complementary to the coding region for synapsin Ia or synaptotagmin I did not overlap with other mammalian sequences determined by a search of the GeneBank/EMBL database.

2.4. Animal care

Animals were maintained in a temperature- and light-controlled environment with 12/12 h light/dark cycle. All experiments were performed in accordance with the Japanese and International Guidelines on the ethical use of animals and all efforts were made to minimize the number of animals used and their suffering.

2.5. Western blot analysis

For quantitation of synaptotagmin I and synapsin I protein levels, rats were anesthetized with 25% urethane and killed by decapitation at various days after a single intraventricular injection of HVJ-liposomes containing the antisense ODNs or reversed antisense ODNs. Hippocampus, neocortex, and striatum were quickly dissected out of removed brain and stored at −80 °C before use, respectively. Tissue was prepared in 0.1 mg/μl of the low-salt lysis buffer (10 mM Tris–HCl (pH 8.0), 0.14 mM NaCl, 3 mM $MgCl_2$, 1 mM dithiothreitol, 1 mM phenylmethylsulphonyl–fluoride and 0.5% (vol/vol) NP-40) and sonicated until the homogenate was uniform. For the detection of synapsin I, tissue was prepared in 0.1 mg/μl solution by the same low-salt lysis buffer containing 0.02 mM calpain inhibitor I, 0.02 mM calpain inhibitor II, 1.6 mM Benzamidine and protease inhibitor mixtures (1:100, Wako Chemical Inc). The homogenate was on ice for 30 min and centrifuged at 12,000 rpm at 4 °C for 10 min. Protein concentration was measured using the bicinchroninic acid protein assay kit (Pierce, Rockford, IL), and protein samples (0.5–1.0 μg) were loaded on 10% (wt./vol) polyacrylamide gel and separated by electrophoresis. Separated proteins were transferred electrophoretically from the gel to a polyvinylidene difluoride (PVDF) membrane (ATTO, Tokyo, Japan). The PVDF membrane was treated with blocking buffer (Block Ace, Dainihon

Seiyaku Inc) at 4 °C overnight, and then incubated with anti-synaptotagmin I antibody (1:1000, Alomon Labs) or anti-synapsin I antibody (1:1000, Alexis Co.) at room temperature for 60 min. After washing with phosphate buffered saline (PBS) containing 0.1% Tween 20, the membrane was treated with peroxidase conjugated anti-rabbit IgG (1:5000, Leinco Technologies) at room temperature for 60 min and enhanced chemiluminescence reagents to visualize the antibody reaction using ECL detection kit (Amersham International, UK) and finally exposed to X ray film (Kodak). To detect syntaxin I protein we used the anti-syntaxin IA antibody (1:20,000, gift from Dr. K. Akagawa (Kushima et al., 1997)) as a primary antibody and we used the peroxidase conjugated anti-mouse IgG (1:10,000, ICN Biomedicals, Inc.) as a secondary antibody. For quantification of protein levels, Western blots were analyzed with computing densitometory by using Scion Image for Windows Beta 4.02 processing and analysis software. Mean optical densities of bands for two samples per animal were determined, and the film background was subtracted. Mean band densities were statistically analyzed with one way ANOVA and post-hoc Fisher's test to determine significance.

2.6. Histology

After survival period of 7 days, post-ischemic rats and matched controls were deeply anesthetized with sodium pentobarbital and their brains were perfused transcardially with phosphate-buffered 4% paraformaldehyde. Brains were removed, postfixed for 1 h in perfusate and saturated in 30% sucrose. The removed brains were cut into coronal sections (10 μm) through the hippocampus by a cryostat. The sections were stained with thionin.

2.7. Quantitative analysis of cell death of hippocampal neurons

To examine the effect of reduced biosynthesis of synaptotagmin I or synapsin I on ischemic cell loss of hippocampal neurons, the survival rate of CA1 and CA3 pyramidal neurons in ischemic rats with or without prior intraventricular injection of the ODNs by using HVJ-liposome method was estimated by the cell density of surviving pyramidal neurons in the CA1 and CA3 regions expressed as a percentage of the averaged cell density of corresponding neurons for non-treated control rats. The cell density was measured by counting the number of Nissl-stained cells per unit volume ($25 \times 100 \times 10\ \mu m^3$) on the CA1 or CA3 layer. Three coronal sections were chosen from three levels of the rostral hippocampus (AP 5.8 mm, AP 5.2 mm, and AP 4.5 mm). To correct for regional differences, the cell density was measured at 20 or 15 points within the CA1 or CA3 sector in both side of one hippocampal section over the three chosen sections of individual rats and then averaged.

3. Results

3.1. Antisense-induced downregulation of synapsin I and synaptotagmin I protein levels in the hippocampus, neocortex and striatum

We first used quantitative Western blot analysis to examine the antisense-induced downregulation of synapsin I or synaptotagmin I protein levels in the hippocampus, neocortex and striatum following a single intraventricular injection of HVJ-liposomes containing antisense ODNs or reversed antisense ODNs.

Fig. 1A shows representative blots obtaind from the hippocampus of non-treated control rats (NT) and treated rats (syn-AS or syn-R) that received an intraventricular injection of syn-AS or syn-R 4 days before the Western blotting assay. As shown in Fig. 1A, the expression of synapsin I protein was downregulated only in the syn-AS treated rat while that of syntaxin I protein was not changed by the syn-AS treatment. Fig. 1B shows representative blots (upper) and quantitation of relative band densities (lower) from the hippocampus, neocortex and striatum of the NT and treated rats (syn-AS or syn-R) that received an intraventricular injection of syn-AS or syn-R 4 days before the Western blotting assay. The expression of synapsin I protein in the hippocampus, neocortex and striatum was downregulated significantly by syn-AS at 4 days after the injection. Fig. 1C shows representative blots (upper) and quantitation of relative band densities (lower) from the hippocampus of the NT and the antisense-treated rats that received an intraventricular injection of syn-AS at 2, 4, 8 and 16 days before the Western blotting assay, respectively. The amount of synapsin I protein in the hippocampus of the syn-AS was downregulated maximally by 56% within 4 days after the injection, and the reduced level was maintained for 4 days until 8 days post-injection and then recovered to the original level up to 16 days post-injection.

Fig. 2A shows representative blots obtained from the hippocampus of NT and treated rats (stm-AS or stm-R) that received an intraventricular injection of stm-AS or stm-R 4 days before the Western blotting assay. As shown in Fig. 2A, the expression of synaptotagmin I protein was downregulated only in the stm-AS treated rat while that of syntaxin I protein was not changed by the stm-AS treatment. Fig. 2B shows representative blots (upper) and quantitation of relative band densities (lower) from the hippocampus, neocortex and striatum of the NT and treated rats (stm-AS or stm-R) that received an intraventricular injection of stm-AS or stm-R 4 days before the Western blotting assay. The

significant reduction of synaptotagmin I expression by intraventricular injection of stm-AS was observed only in the hippocampus at 4 days after the injection. Fig. 2C shows representative blots (upper) and quantitation of relative band densities (lower) from the hippocampus of the NT and the antisense-treated rats (stm-AS) that received an intraventricular injection of stm-AS at 2, 4, 8 and 16 days before the Western blotting assay, respectively. The amount of synaptotagmin I protein in the hippocampus of the stm-AS was downregulated by 29% within 4 days post-injection, and the reduced level was maintained for 4 days until 8 days post-injection and then recovered to the original level up to 16 days after the injection.

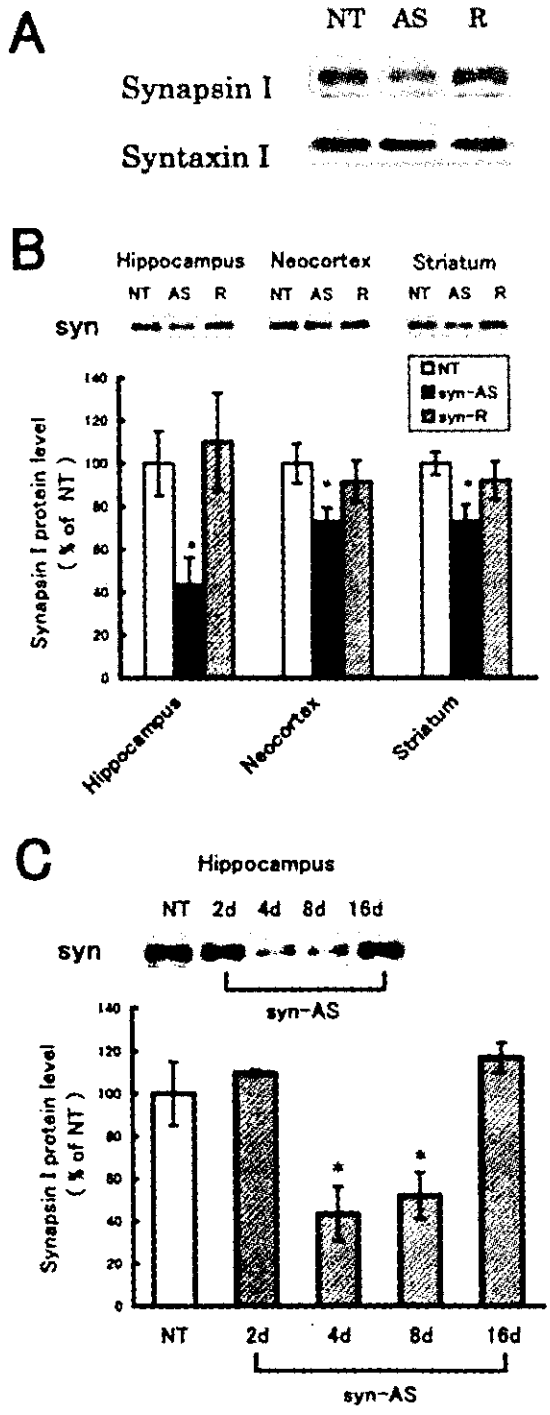

Fig. 1

3.2. Modulation of ischemic damage of hippocampal neurons in rats with antisense in vivo knockdown of synaptotagmin I or that of synapsin I

In ischemic rats with prior intraventricular injection of stm-AS by using HVJ-liposome gene transfer method, all pyramidal neurons in the overall layers of hippocampus remained intact, indicating that the ischemic neuron loss of CA1 pyramidal neurons was completely prevented by the prior treatment with stm-AS (Fig. 3G–I), when compared with the ischemic damage of pyramidal neurons observed exclusively in the CA1 layer in ischemic rats without any prior treatment (Fig. 3D–F). On the other hands, in ischemic rats with prior intraventricular injection of syn-AS by HVJ-liposome gene transfer method, the deterioration of ischemic damage of CA1 pyramidal neurons was observed and the neuron loss also became apparent in the CA2 and CA3 regions which were relatively resistant to ischemia (Fig. 3J–L), showing that the syn-AS treatment markedly promoted the evolution of ischemic damage of pyramidal neurons in the entire hippocampus.

As a control for a specific action of stm-AS or syn-AS on the ischemic brain damage, we used stm-R or syn-R, respectively. In ischemic rats with prior intraventricular injection of stm-R by HVJ-liposome gene transfer method, ischemic damage of CA1 pyramidal neurons

Fig. 1. Downregulation of synapsin I (syn) protein levels in the hippocampus induced by a single intraventricular injection of HVJ-liposome suspension containing antisense ODNs against synapsin I (syn-AS). (A) Representative blots for synapsin I and syntaxin I proteins obtained from the hippocampus of non-treated control rats (NT) and treated rats (syn-AS or syn-R) that received an intraventricular injection of syn-AS or reversed antisense ODNs (syn-R) 4 days prior to the Western blotting assay. (B) Representative blots (upper) and quantification of relative band densities (lower) from the hippocampus, neocortex and striatum of NT and syn-AS or syn-R rats that received an intraventricular injection of syn-AS or syn-R 4 days prior to the Western blotting assay. (C) Representative blots (upper) and quantification of relative band densities (lower) from the hippocampus of the NT and the syn-AS treated rats that received an intraventricular injection of syn-AS at 2 days (2 d), 4 days (4 d), 8 days (8 d) or 16 days (16 d) prior to the Western blotting assay. Each averaged band density from treated rats ($n = 4$) was represented as a percentage of that of the NT ($n = 4$) (mean ± S.E.M.). * Significantly different from the NT by ANOVA and post-hoc Fisher's test ($P < 0.05$).

in the hippocampus was rather attenuated, showing a considerable increase in the number of surviving CA1 neurons (Fig. 4A–C) when compared with that in ischemic rats without any prior treatment (Fig. 3D–F). In rats with prior intraventricular injection of syn-R by HVJ-liposome gene transfer method, apparent attenuation of the ischemic damage of hippocampal CA1 neurons was also observed (Fig. 4D–F), which was quite similar to the outcome with the stm-R treatment.

As demonstrated in Fig. 5A, a single intraventricular injection of stm-AS by using HVJ-liposome method 4 days prior to a transient ischemia caused almost complete prevention of the ischemia-induced neuron loss of CA1 pyramidal neurons which were most vulnerable to ischemia, increasing the survival rate of CA1 neurons from 45 up to 91% by 46%. On the other hands, a single intraventricular injection of syn-AS by HVJ-liposome method markedly promoted the evolution of the ischemic damage of CA1 pyramidal neurons, reducing the survival rate of CA1 neurons from 45 to 17% by 28%. As for the treatment with the reversed antisense as a control, a single intraventricular injection of stm-R by using HVJ-liposome method 4 days prior to a transient ischemia attenuated significantly the ischemic damage, increasing the survival rate of CA1 neurons from 45 to 66% by 21%. The same treatment with syn-R also caused the significant attenuation of the ischemic damage of CA1 neurons, increasing the survival rate of CA1 neurons by 26% compared with that (45%) in the ischemic rats without any prior treatment.

As demonstrated in Fig. 5B, only a single intraventricular injection of syn-AS by HVJ-liposome method 4 days prior to a transient ischemia caused the significant enhancement of the ischemic damage of CA3 pyramidal neurons in the hippocampus which were relatively resistant to ischemia, reducing the survival rate of CA3 neurons by 21%, compared with that (90%) in the ishemic rats without any prior treatment. The prior treatment with stm-AS, stm-R or syn-R did not affect the survival rate of CA3 pyramidal neurons.

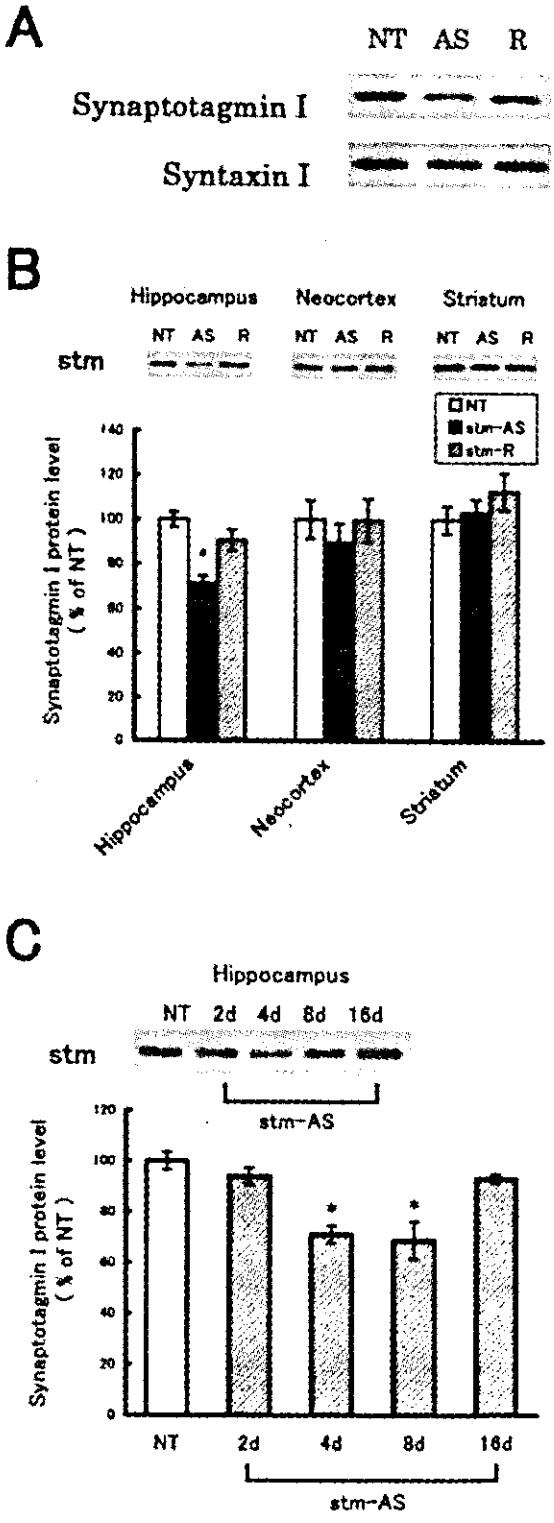

Fig. 2

Fig. 2. Downregulation of synaptotagmin I (stm) protein levels in the hippocampus induced by a single intraventricular injection of HVJ-liposome suspension containing antisense ODNs against synaptotagmin I (stm-AS). (A) Representative blots for synaptotagmin I and syntaxin I proteins obtained from the hippocampus of non-treated control rats (NT) and treated rats (stm-AS or stm-R) that received an intraventricular injection of stm-AS or reversed antisense ODNs (stm-R) 4 days prior to the Western blotting assay. (B) Representative blots (upper) and quantification of relative band densities (lower) from the hippocampus, neocortex and striatum of NT and stm-AS or stm-R rats that received an intraventricular injection of stm-AS or stm-R 4 days prior to the Western blotting assay. (C) Representative blots (upper) and quantification of relative band densities (lower) from the hippocampus of the NT and the stm-AS treated rats that received an intraventricular injection of stm-AS at 2 days (2 d), 4 days (4 d), 8 days (8 d) or 16 days (16 d) prior to the Western blotting assay. Each averaged band density from treated rats ($n = 4$) was represented as a percentage of that of the NT ($n = 4$) (mean $\pm$ S.E.M.). * Significantly different from the NT by ANOVA and post-hoc Fisher's test ($P < 0.01$).

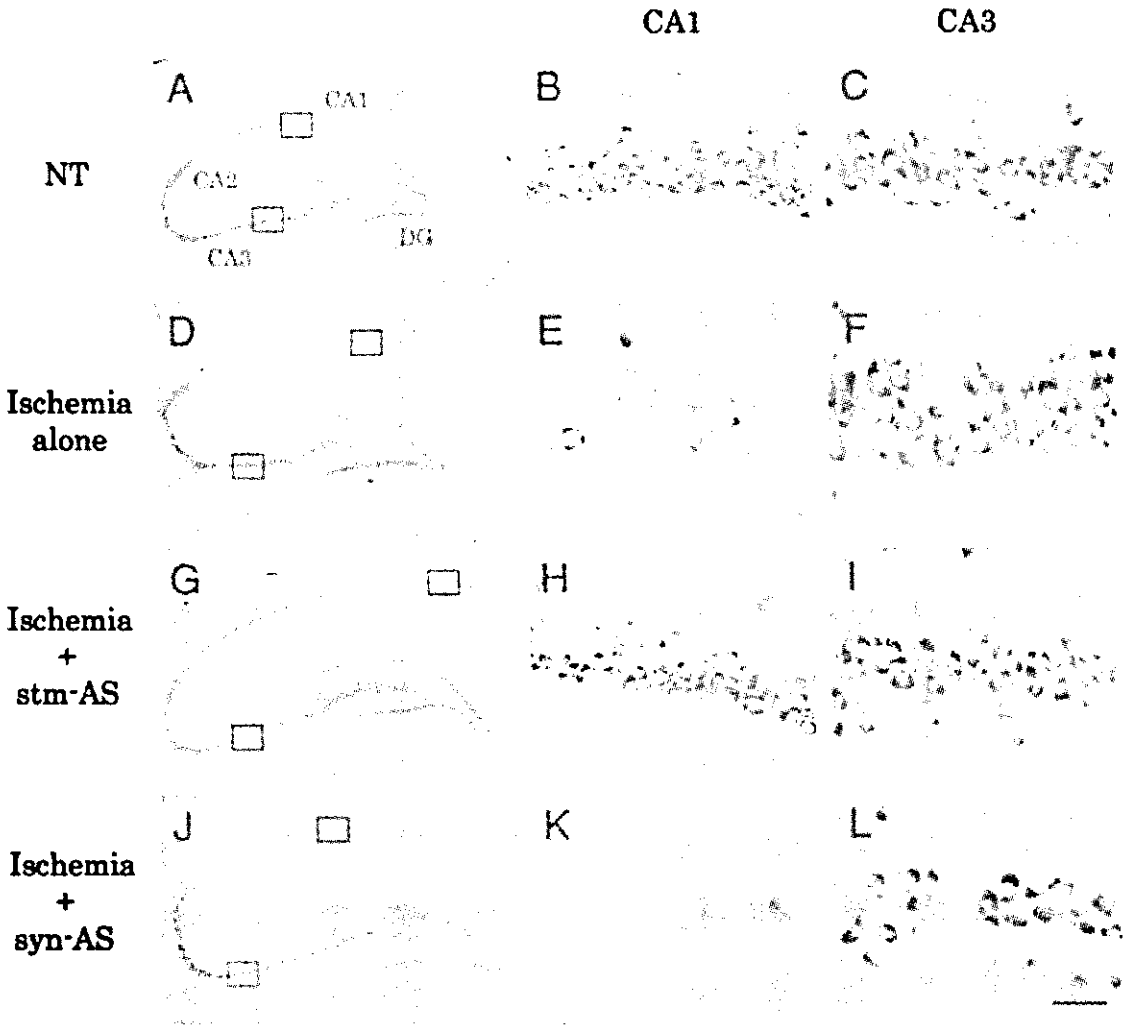

Fig. 3. Effect of the intraventricular injection of antisense ODNs against synaptotagmin I (stm-AS) or antisense ODNs against synapsin I (syn-AS) on the ischemia-induced damage of pyramidal neurons in the hippocampus 7 days after the transient forebrain ischemia of 20 min. (A) Nissl-stained section of the hippocampus of the non-treated control rat (NT). (B,C) Enlarged view of intact CA1 neurons (B) and CA3 neurons (C) from the area indicated by a square in (A). (D) Nissl-stained section of the hippocampus of the ischemic rat without any prior treatment (ischemia alone), indicating the severe damage of pyramidal neurons occurred uniformly over the CA1 sector. (E,F) Enlarged view of damaged CA1 neurons (E) and CA3 neurons (F) from the area indicated by a square in (D). (G) Nissl-stained section of the hippocampus of the ischemic rat with a prior inraventricular injection of stm-AS (ischemia+stm-AS) by using HVJ-liposome method, demonstrating the almost complete rescue of CA1 pyramidal neurons from the ischemic neuron death. (H,I) Enlarged view of the rescued CA1 neurons (H) and intact CA3 neurons (I) from the area indicated by a square in (G). (J) Nissl-stained section of the hippocampus of the ischemic rat with prior intraventricular injection of syn-AS (ischemia+syn-AS) by using HVJ-liposome method, showing the almost complete loss of CA1 pyramidal neurons and severe damage of CA3 pyramidal neurons. (K,L) Enlarged view of complete loss of CA1 neurons (K) and severe damage of CA3 neurons (L) indicated by a square in (J). Scale bar: 550 μm for A, D, G, J and 50 μm for B, C, E, F, H, I, K, L.

3.3. Behavioral observations of rats with the antisense ODNs treatment before and after the ischemic insult

Before and after the ischemic insult, none of the animals treated with a single intraventricular injection of stm-AS or syn-AS by using HVJ-liposome method exhibited abnormality in behaviors like spontaneous occurrence of certain type of epileptic seizures including subconvulsive automatisms or convulsive seizures, hyperactive locomotion, defective adaptation, depressed moving or lack of eating and drinking.

4. Discussion

Western blot analysis revealed that a single intraventricular injection of stm-AS–HVJ-liposome complex and syn-AS–HVJ-liposome complex caused a 30%

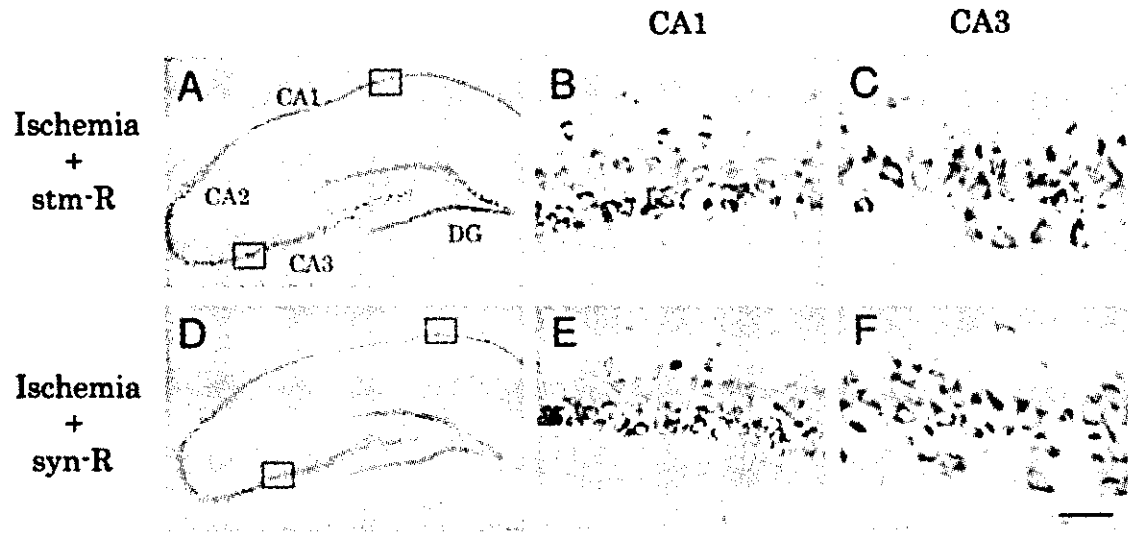

Fig. 4. Effect of the intraventricular injection of reversed antisense against synaptotagmin I (stm-R) and reversed antisense ODNs against synapsin I (syn-R) on the ischemia-induced damage of pyramidal neurons in the hippocampus 7 days after the transient forebrain ischemia of 20 min. (A) Nissl-stained section of the hippocampus of the ischemic rat with a prior intraventricular injection of stm-R (ischemia+stm-R) by using HVJ-liposome method, showing the rather attenuated damage of CA1 pyramidal neurons. (B,C) Enlarged view of surviving CA1 neurons with slight to mild neuron loss (B) and intact CA3 neurons (C) from the area indicated by a square in (A). (D) Nissl-stained section of the hippocampus of the ischemic rat with a prior intraventricular injection of syn-R (ischemia+syn-R), indicating the rather attenuated damage of CA1 pyramidal neurons. (E,F) Enlarged view of surviving CA1 neurons with mild neuron loss (E) and intact CA3 neurons (F) indicated by a square in (D). Scale bar: 550 μm for A, D and 50 μm for B, C, E, F.

inhibition of synaptotagmin I expression and 56% inhibition of synapsin I expression in the hippocampus for more than a week, respectively (see Figs. 1 and 2). The blocking effect of this intraventricular injection of antisense ODNs by HVJ-liposome method on the biosynthesis of synaptotagmin I or synapsin I and the long-lasting action of antisense ODNs are equal to those of chronic infusion by osmotic pump of the antisense ODNs to NMDA receptor subunit NR1 into the lateral ventricle (Wahlestedt et al., 1993). Because of a single injection of the antisense ODNs–HVJ-liposome suspension without any stressful implantation of cannula for repeated or chronic infusion into the brain, this combined use of the antisense technique and HVJ-liposome-mediated gene transfer is thought to be a suitable therapeutic way to attenuate or prevent the brain injury in acute neurodegenerative disorders such as forebrain ischemia or status epilepticus.

A large volume of evidence has accumulated to indicate that synaptotagmin I plays a regulatory role in promoting evoked transmitter release through interaction with the fusion machinery (Leveque et al., 1992; Geppert et al., 1994; Mikoshiba et al., 1995; Popoli et al., 1997; Littleton et al., 2001). In particular, synaptotagmin I mutants in Drosophila revealed profound defects in neurotransmitter release including a severe reduction in evoked release, an increase in spontaneous fusion and delays in the onset of vesicle fusion (Littleton et al., 1993, 1994; DiAntonio et al., 1993). In mutant mice lacking synaptotagmin I, the mutation resulted in the selective loss of the rapid synchronous exocytosis without affecting the frequency of spontaneous fusion events (Geppert et al., 1994). As post-ischemic neuroprotection by glutamate receptor antagonist (Sheardown et al., 1990, Nellgard and Wieloch, 1992; Sheardown et al., 1993) and rescue of CA1 pyramidal neurons from ischemic damage by surgical removal of CA3 projection fibers (Wieloch et al., 1985; Onodera et al., 1986; Jorgensen et al., 1987; Buchan and Pulsinelli, 1990) have suggested, glutamate release from synaptic terminals during and after the ischemic insult is thought to be essential for glutamate receptor-mediated excitotoxicity in ischemic brain injury. Furthermore, the majority of excitatory synapses in the central nervous system is thought to be glutamatergic. Considering together, it has been predicted that the antisense-induced downregulation of synaptotagmin I causes attenuation or prevention of ischemic damage of hippocampal neurons probably by reduced rates of transmitter release at terminals. As we predicted, the antisense-induced knockdown of synaptotagmin I expression in the whole brain completely prevented the ischemic delayed cell death of hippocampal CA1 neurons in this experiment (see Figs. 3 and 5). This observation strongly suggests that reduction of evoked exocytotic release of transmitter from excitatory synaptic terminals, in particular glutamate release, may be involved in neuroprotection afforded by antisense in vivo knockdown of synaptotagmin I, although the same antisense treatment has not induced any abnormal

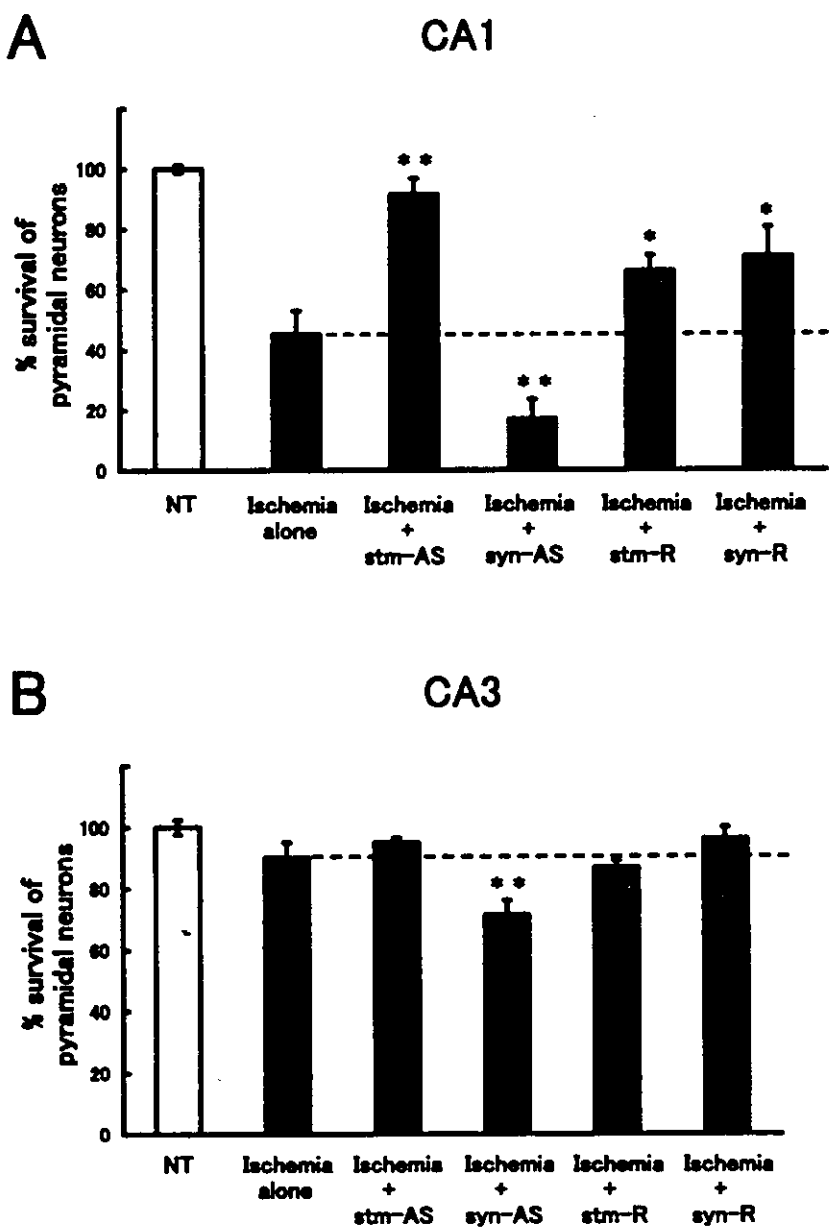

Fig. 5. Quantitative analysis for the effect of the prior intraventricular injection of antisense ODNs (stm-AS, syn-AS) and reversed antisense ODNs (stm-R, syn-R) by using HVJ-liposome method on the ischemic damage of pyramidal neurons in the CA1 (A) and CA3 (B) region in the hippocampus, 7 days after the transient forebrain ischemia of 20 min. The survival rate of pyramidal neurons was estimated by the cell density of surviving neurons in the CA1 and CA3 pyramidal layer expressed as a percentage of the averaged cell density of pyramidal neurons in corresponding region for the non-treated control rats. Treatment for each group was: NT ($n = 11$), non-treated control rat; ischemia alone ($n = 14$), ischemic rat without any prior treatment; ischemia+stm-AS ($n = 12$), ischemic rat with a prior intraventricular injection of stm-AS; ischemia+syn-AS ($n = 7$), ischemic rat with a prior intraventricular injection of syn-AS; ischemia+stm-R ($n = 9$); ischemic rat with a prior intraventricular injection of stm-R; ischemia+syn-R ($n = 6$), ischemic rat with a prior intraventricular injection of syn-R. The values were mean ± S.E.M. * Significantly different from the Ischemia alone ($P < 0.05$); ** Significantly different from the ischemia alone ($P < 0.01$), by ANOVA and post-hoc Fisher's test.

behaviors which reflect defects in sensory motor function due to dysfunction of synaptic transmission.

Our present study also demonstrated that antisense in vivo knockdown of synapsin I rather promoted the evolution of the ischemic neuron damage in the hippocampus, resulting in almost complete neuron loss of CA1 pyramidal neurons and mild to severe damage of relatively resistant CA2 and CA3 pyramidal neurons (see Figs. 3 and 5). Chi et al. have revealed the involvement of synapsins in neurotransmitter release; that is, the synapsin, a family of highly conserved protein associated with synaptic vesicles, acts as a

phosphorylation-dependent regulator of synaptic vesicle mobilization and hence neurotransmission (Chi et al., 2001), controlling the synaptic vesicle life cycle via dissociation–reassociation cycle of synapsins with vesicles depended on synaptic activity (Murthy, 2001). From this possible role of synapsin I, it has been postulated that antisense in vivo knockdown of synapsin I induces a slowed turnover of synaptic vesicle and thereby reduced rates of evoked transmitter release at the presynaptic nerve terminals. Our present observation seems to be inconsistent with this predicted reduction of transmitter release by antisense-induced downregulation of synapsin I expression at overall presynaptic terminals. Contrary to expected role of synapsins in transmitter release, synapsin mutant mice can survive without any appreciable defect in morphology of the brain or general behavior, although some subtle perturbations in electrophysiological responses that are difficult to interpret occur. The only apparent abnormality in synapsin I mutant mice was late onset epileptic seizures and stimulation-evoked seizures (experimental temporal lobe epilepsy) (Rosahl et al., 1993, 1995; Li et al., 1995; Takei et al., 1995). Recently, Terada et al. have provided a new insight into the epileptic seizure susceptibility occurring in the synapsin I mutant mice; in the cultured hippocampal synapses from mutant mice lacking synapsin I, repeated application of a hypertonic solution to hippocampal synapses suppressed the subsequent transmitter release, associated with an accelerated vesicle replenishing time at the inhibitory synapses, but not at the excitatory synapses (Terada et al., 1999), indicating that synapsin I at the inhibitory synapses plays a crucial role in minimizing transmitter depletion. This finding suggests that defect in turnover rate of synaptic vesicle at inhibitory synapses but not at excitatory synapses can produce disintegration of certain neural circuits such as the limbic system, culminating in spontaneous epileptic seizure presumably due to removal of GABAergic inhibitory neurotransmission. Therefore, considering this finding, our result may suggest that the marked enhancement of ischemic damage of hippocampal neurons observed in rats with synapsin knockdown can be interpreted as an outcome of increased excitability of the hippocampus by disintegration of limbic circuitry due to attenuation of inhibitory neurotransmission (disinhibition), although the rats with antisense in vivo knockdown (56%) of synapsin I did not exhibit seizure susceptibility. Indeed, the deterioration of ischemic damage of pyramidal neurons by synapsin I antisense occurred in the entire hippocampus including CA2/CA3 pyramidal neurons relatively resistant to ischemia, supporting this interpretation. As for alternative interpretation, the postsynaptic modulation of neurotransmission by synapsin I knockdown such as defects in clustering or insertion of receptors and channels in postsynaptic membrane is quite unlikely, because synapsins are abundant in presynaptic nerve terminals and act mainly as a regulatory factor related to vesicle trafficking at presynaptic terminals (Llinas et al., 1985; Hirokawa et al., 1989; Ceccaldi et al., 1995; Pieribone et al., 1995).

In this study, our result showed that prior intraventricular treatment with reversed antisense to synaptotagmin I (stm-R) and that to synapsin I (syn-R) by using HVJ-liposome method attenuated ischemia-induced damage of hippocampal CA1 neurons by 21–26%, while the same treatment did not affect the survival rate of CA3 neurons (see Figs. 4 and 5). The similar neuroprotection was observed in ischemic rats with prior intraventricular injection of HVJ-liposome containing mismatched antisense ODNs or HVJ-liposome containing vehicle BSS (data not shown). This neuroprotective effect of the stm-R- or syn-R–HVJ-liposome complex on the ischemic cell death of CA1 neurons seems to be unexpected and difficult to explain. Contrary to our result, the intraventricular infusion of the sense- or random-ODNs against NMDA receptor has not caused this type of neuroprotective effects on the ischemic brain injury in rats (Wahlestedt et al., 1993). As the neuroprotection observed in rats treated with stm-R–HVJ-liposome complex is quite similar to that with syn-R–HVJ-liposome complex, the action of the ODNs–HVJ-liposome complex is thought to be of nonspecific, not depending on the sequences of ODNs. Therefore, one interpretation for this nonspecific neuroprotection may be an outcome of toxic actions of HVJ-liposome vector to host cells probably via HVJ-mediated agitation in ionic homeostasis, resulting in lowered cellular metabolism (Saeki and Kaneda, 1998). Considering this nonspecific action of HVJ-liposome itself, the synergestic action of antisense ODNs to synaptotagmin I and HVJ-liposome vector may reflect a complete prevention of ischemia-induced cell death of hippocampal neurons by the intraventricular injection of the stm-AS–HVJ-liposome suspension observed in the present study.

Acknowledgements

This study was supported by the grant-in-aid for Scientific Research (no. 13670665) from the Ministry of Education, Science and Culture, Japan, and the Health Sciences Research Grants (no. H12-brain-018) from the Ministry of Health, Labor and Welfare, Japan. This investigation was also supported in part by the Grant for Scientific Research from Kitasato University Graduate School of Medical Science, Japan. We thank Dr. K. Akagawa for kindly giving us antibody against syntaxin IA.

References

Benveniste, H., Jorgensen, M.B., Sandberg, M., Christensen, T., Hagberg, H., Diemer, N.H., 1989. Ischemic damage in hippocampal CA1 is dependent on glutamate release and intact innervation from CA3. J. Cereb. Blood Flow Metab. 9, 629–639.

Bommert, K., Charlton, M.P., DeBello, W.M., Chin, G.J., Betz, H., Augastine, G.L., 1993. Inhibition of neurotransmitter release by C2-domain peptides implicates synaptotagmin in exocytosis. Nature 363, 163–165.

Buchan, A.M., Pulsinelli, W.A., 1990. Septo-hippocampal deafferentation protects CA1 neurons against ischemic injury. Brain Res. 512, 7–14.

Ceccaldi, P.-E., Grohoraz, F., Benfenati, F., Chieregatti, E., Greengard, P., Valtorta, F., 1995. Dephosphorylated synapsin I anchors synaptic vesicles to actin cytoskeleton: an analysis by videomicroscopy. J. Cell Biol. 128, 905–912.

Chi, P., Greegard, P., Ryan, T.A., 2001. Synapsin dispersion and reclustering during synaptic activity. Nat. Neurosci. 4, 1187–1193.

De Keyser, J., Sulter, G., Luiten, P.G., 1999. Clinical trials with neuroprotective drugs in acute ischemic stroke: are we doing the right thing? Trends Neurosci. 12, 535–540.

DiAntonio, A., Parfitt, K.D., Schwarz, T.L., 1993. Synaptic transmission persists in synaptotagmin mutants of *Drosophila*. Cell 73, 1281–1290.

Geppert, M., Goda, Y., Hammer, R.E., Li, C., Rosahl, T.W., Stevens, C.F., Sudhof, T.C., 1994. Synaptotagmin I: a major Ca^{2+} sensor for transmitter release at a central synapse. Cell 79, 717–727.

Hilfiker, S., Schweizer, F.E., Kao, H.-T., Czernik, A.J., Greengard, P., Augastine, G.J., 1998. Two sites of action for synapsin domain E in regulating neurotransmitter release. Nat. Neurosci. 1, 29–35.

Hirokawa, N., Sobue, K., Kaneda, K., Harada, A., Yorifuji, H., 1989. The cytoskeletal architecture of the presynaptic terminal and molecular structure of synapsin I. J. Cell Biol. 108, 111–126.

Hosaka, M., Hammer, R., Sudhof, T.C., 1999. A phospho-switch controls the dynamic association of synapsins with synaptic vesicles. Neuron 24, 377–387.

Jorgensen, M., Johansen, F., Diemer, N., 1987. Removal of the entorhinal cortex protects hippocampal CA-1 neurons from ischemic damage. Acta Neuropathol. 73, 189–194.

Kaneda, Y., Iwai, K., Uchida, T., 1989. Increased expression of DNA cointroduced with nuclear protain in adult rat liver. Science 243, 375–378.

Kimura, M., Saji, M., 1997. Protective effect of a low dose of colchicine on the delayed cell death of hippocampal CA1 neurons following transient forebrain ischemia. Brain Res. 774, 229–233.

Kushima, Y., Fujiwara, T., Sanada, M., Akagawa, K., 1997. Characterization of HPC1-antigen, an isoform of syntaxin-1, with the isoform-specific monoclonal antibody, 14D8. J. Mol. Neurosci. 8, 19–27.

Leveque, C., Hoshino, T., David, P., Shoji-Kasai, Y., Leys, K., Omori, A., Lang, B., El Far, O., Sato, K., Martin-Moutot, N., Newsom-Davis, J., Takahashi, M., Seagar, M.J., 1992. The synaptic vesicle protein synaptotagmin associates with calcium channels and is a putative Lambert–Eaton myasthenic syndrome antigen. Proc. Natl. Acad. Sci. USA 89, 3625–3629.

Li, L., Chin, L.-S., Shupliakov, O., Brodin, L., Sihra, T.S., Hvalby, O., Jensen, V., Zheng, D., McNamara, J.O., Greengard, P., Andersen, P., 1995. Impairment of synaptic vesicle clustering and of synaptic transmission, and increased seizure propensity, in synapsin I-deficient mice. Proc. Natl. Acad. Sci. USA 92, 9235–9239.

Littleton, J.T., Stern, M., Schulze, K., Perin, M., Bellen, H.J., 1993. Mutational analysis of *Drosophila synaptotagmin* demonstrates its essential role in Ca^{2+}-activated neurotransmitter release. Cell 74, 1125–1134.

Littleton, J.T., Stern, M., Perin, M., Bellen, H.J., 1994. Calcium dependence of neurotransmitter release and rate of spontaneous vesicle fusions are altered in *Drosophila synaptotagmin* mutants. Proc. Natl. Acad. Sci. USA 91, 10888–10892.

Littleton, J.T., Bai, J., Vyas, B., Desai, R., Baltus, A.E., Garment, M.B., Carlson, S.D., Ganetzky, B., Chapman, E.R., 2001. Synaptotagmin mutants reveal essential functions for the C2B domain in Ca^{2+}-triggered fusion and recycling of synaptic vesicles in vivo. J. Neurosci. 21, 1421–1433.

Llinas, R., McGuinness, T.L., Leonard, C.S., Sugimori, M., Greengard, P., 1985. Intraterminal injection of synapsin I or calcium/calmodulin-dependent protain kinase II alters neurotransmitter release at the squid giant synapse. Proc. Natl. Acad. Sci. USA 82, 3035–3039.

Mikoshiba, K., Fukuda, M., Moreira, J.E., Lewis, F.M.T., Sugimori, M., Ninobe, M., Llinas, R., 1995. Role of the C2A domain of synaptotagmin in transmitter release as determined by specific antibody injection into the squid giant synapse preterminal. Proc. Natl. Acad. Sci. USA 92, 10703–10707.

Morishita, R., Gibbons, G.H., Kaneda, Y., Ogihara, T., Dzau, V.J., 1994. Pharmacokinetics of antisense oligodeoxynucleotides (cyclin B_1 and CDC2 kinase) in the vessel wall in vivo: enhanced therapeutic utility for restenosis by HVJ-liposome delivery. Gene 149, 13–19.

Murthy, V.N., 2001. Spreading synapsins. Nat. Neurosci. 4, 1154–1157.

Nellgard, B., Wieloch, T., 1992. Postischemic blockade of AMPA but not NMDA receptors mitigates neuronal damage in the rat brain following transient severe cerebral ischemia. J. Cereb. Blood Flow Metab. 12, 2–11.

Nonet, M.L., Grundahl, K., Meyer, B.J., Rand, J.B., 1993. Synaptic function is impaired but not eliminated in *C. elegans* mutants lacking synaptotagmin. Cell 73, 1291–1305.

Onodera, H., Sato, G., Kogure, K., 1986. Lesions to Schaffer collatrals prevent ischemic death of CA1 pyramidal cells. Neurosci. Lett. 68, 169–174.

Perin, M.S., Fried, V.A., Mignery, G.A., Jahn, R., Sudhof, T.C., 1990. Phospholipid binding by a synaptic vesicle protein homologous to the regulatory region of protein kinase C. Nature 345, 260–263.

Pieribone, V.A., Shupliakov, O., Brodin, L., Hilfiker-Rothenfluh, S., Czernik, A.J., Greengard, P., 1995. Distinct pools of synaptic vesicles in neurotransmitter release. Nature 375, 493–497.

Popoli, M., Venegoni, A., Buffa, L., Racagni, G., 1997. Ca^{2+}/phospholipid-binding and syntaxin-binding of native synaptotagmin I. Life Sci. 61, 711–721.

Pulsinelli, W.A., Brierley, J.B., 1979. A new model of bilateral hemispheric ischemia in the unanesthetized rat. Stroke 10, 267–272.

Rosahl, T.W., Geppert, M., Spillane, D., Herz, J., Hammer, R.E., Malenka, R.C., Sudhof, T.C., 1993. Short-term synaptic plasticity is altered in mice lacking synapsin I. Cell 75, 661–670.

Rosahl, T.W., Spillane, D., Missler, M., Herz, J., Selig, D.K., Wolff, J.R., Hammer, R.E., Malenka, R.C., Sudhof, T.C., 1995. Essential functions of synapsins I and II in synaptic vesicle regulation. Nature 375, 488–493.

Saeki, Y., Kaneda, Y., 1998. Protain modified liposomes (HVJ-liposomes) for the delivery of genes, oligonucleotides and proteins. In: Celis, J.E. (Ed.), Cell Biology: a Laboratory Handbook, vol. 4. Academic Press, San Diego, pp. 127–135.

Saji, M., Cohen, M., Blau, A.D., Wessel, T.C., Volpe, B.T., 1994. Transient forebrain ischemia induces delayed injury in the substantia nigra reticulata: degeneration of GABA neurons, compensatory expression of GAD mRNA. Brain Res. 643, 234–244.

Sheardown, M.J., Nielsen, E.O., Hansen, A.J., Jacobsen, P., Honore, T., 1990. 2,3-Dihydroxy-6-nitro-7-sulfamoyl-benzo(F)quinoxaline: a neuroprotectant for cerebral ischemia. Science 247, 571–574.

Sheardown, M.J., Suzdak, P.D., Nordholm, L., 1993. AMPA, but not NMDA, receptor antagonism is neuroprotective in gerbil global ischaemia, even when delayed 24 h. Eur. J. Pharmacol. 236, 347–353.

Takei, Y., Harada, A., Takeda, S., Kobayashi, K., Terada, S., Noda, T., Takahashi, T., Hirokawa, N., 1995. Sinapsin I deficiency results in the structural change in the presynaptic terminals in the murine nervous system. J. Cell Biol. 131, 1789–1800.

Terada, S., Tsujimoto, T., Takei, Y., Takahashi, T., Hirokawa, N., 1999. Impairment of inhibitory synaptic transmission in mice lacking synapsin I. J. Cell Biol. 145, 1039–1048.

Tomita, N., Higaki, J., Morishita, R., Kato, K., Mikami, H., Kaneda, Y., Ogihara, T., 1992. Direct in vivo gene introduction into rat kidney. Biochem. Biophys. Res. Commun. 186, 129–134.

Wahlestedt, C., Golanov, E., Yamamoto, S., Yee, F., Ericson, H., Yoo, H., Inturrisi, C.E., Reis, D.J., 1993. Antisense oligodeoxynucleotides to NMDA-R1 receptor channel protect cortical neurons from excitotoxicity and reduce focal ischaemic infarctions. Nature 363, 260–263.

Wieloch, T., Lindvall, O., Blomqvist, P., Gage, F.H., 1985. Evidence for amelioration of ischemic neuronal damage in the hippocampal formation by lesions of the perforant path. Neurol. Res. 7, 24–26.

Yamada, K., Moriguchi, A., Morishita, R., Aoki, M., Nakamura, Y., Mikami, H., Oshima, T., Ninomiya, M., Kaneda, Y., Higaki, J., Ogihara, T., 1996. Efficient oligonucleotide delivery using thr HVJ-liposome method in the central nervous system. Am. J. Physiol. 271, R1212–R1220.

Zurmohle, U., Herms, J., Schlingensiepen, R., Brysch, W., Schlingensiepen, K.H., 1996. Changes in the expression of synapsin I and II messenger RNA during postnatal rat brain development. Exp. Brain Res. 108, 441–449.

小児医学の最近の進歩

ライソゾーム病に対するケミカルシャペロン療法

鈴木義之*

要旨

脳の遺伝病に対する新しい治療法（ケミカルシャペロン療法）の開発の試みを行った．その考え方を解説し，疾患モデルとしての遺伝性ライソゾーム病，G_{M1}-ガングリオシドーシスの治療実験データを提示した．ガングリオシド G_{M1} の側鎖末端にあるガラクトースに類似の低分子化合物 NOEV が，試験管内で β-ガラクトシダーゼを競合的に阻害し，細胞内で変異蛋白質を安定化し，ライソゾームの酸性環境で解離した変異分子の酵素活性を発現させた．ヒト患者やモデルマウス由来の培養細胞，モデルマウス個体で，NOEV が変異酵素活性を上昇させ，蓄積基質を分解することを確認した．この方法は，ライソゾーム病ばかりでなく，多くの脳の遺伝病に対する新しい治療法となる可能性がある．

はじめに——シャペロンとは

日本では，シャペロンという用語は一般にはあまり知られておらず，なじみのない医師も少なくないと思う．そこで，この言葉の説明から始めることにする．

広辞苑や世界大百科事典など，国内の一般的な辞書，事典類にはこの項目はない．英語圏でもっとも権威のある Oxford English Dictionary（OED）第2版（1989年）を見ると以下の順序で解説されている．貴族(14世紀)，後には貴婦人(16世紀)のかぶる頭巾，帽子．ガーター勲位の装束の一部(16世紀)，棺を引く馬の前頭部につける飾り（17世紀），などの意味を経て，若い未婚の女性が社交界に出るときの付き添い(多くは年配の既婚女性)で，主に行儀作法を指導し監督する人(18世紀)，などの意味に使われたとの説明がある．

そして現在の臨床医学では，医師とは異なった性の患者を診察するときに医師に付き添う人，という意味で使われる(Stedman's Medical Dictionary, 27 th ed, 2000)．筆者も米空軍病院でのインターン時代，女性の診察をするのに，忙しい時間帯に看護婦さんに立ち会ってもらうために，ずいぶん待たされていらいらしたことを今でも覚えている．

最近になって，これらの一般的な用法に加えて，生物学では分子シャペロンという言葉が使われることが多くなった．多くの生物学辞典，理化学辞典，医学辞典には「他の蛋白質や蛋白質複合体の適正な折りたたみや構築を行う別の蛋白質」という定義が記載されている．単にシャペロンともいう．細胞内で熱変性を予防し，蛋白質が正しく働く機能を介助する熱ショック蛋

* Yoshiyuki SUZUKI 国際医療福祉大学臨床医学研究センター
[連絡先] 〒324-8501 栃木県大田原市北金丸2600-1 国際医療福祉大学臨床医学研究センター